



HAL
open science

Heterogeneous crystal and poly-crystal plasticity modeling from a transformation field analysis within a regularized Schmid law

Patrick Franciosi, Stéphane Berbenni

► **To cite this version:**

Patrick Franciosi, Stéphane Berbenni. Heterogeneous crystal and poly-crystal plasticity modeling from a transformation field analysis within a regularized Schmid law. *Journal of the Mechanics and Physics of Solids*, 2007, 55 (11), pp.2265-2299. 10.1016/j.jmps.2007.04.012 . hal-03619985

HAL Id: hal-03619985

<https://hal.science/hal-03619985>

Submitted on 25 Mar 2022

HAL is a multi-disciplinary open access archive for the deposit and dissemination of scientific research documents, whether they are published or not. The documents may come from teaching and research institutions in France or abroad, or from public or private research centers.

L'archive ouverte pluridisciplinaire **HAL**, est destinée au dépôt et à la diffusion de documents scientifiques de niveau recherche, publiés ou non, émanant des établissements d'enseignement et de recherche français ou étrangers, des laboratoires publics ou privés.

Heterogeneous crystal and poly-crystal plasticity modeling from a transformation field analysis within a regularized Schmid law

P. Franciosi^{a,*}, S. Berbenni^b

^a*LPMTM, UPR9001 CNRS, Institut Galilée, University of Paris 13, 93430 Villetaneuse, France*

^b*LPMM, UMR7554 CNRS, University of Metz Technopole, 57078 Metz Cedex 03, France*

Abstract

The regularized Schmid law (RSL) has recently been proposed as a plastic flow criterion for poly-crystals under the crude assumptions of either uniform stress or uniform strain. We first reconsider this law for application to heterogeneous intra-crystalline plasticity, with reference to a Homogeneous Equivalent Super-Crystal. We then extend the modeling to poly-crystals with the goal to account for both stress and strain heterogeneities within as well as between grains. The transformation field analysis (TFA) is used as the homogenization procedure. This TFA is known to be accurate for materials that can be described as assemblies of plastically homogeneous domains. Otherwise, the estimates of the material effective behavior that result from its application are too stiff. Because stress and strain fields are almost everywhere uniform in laminates, we consider crystal slip organizations into multi-laminate structures. It is demonstrated that laminate layers either parallel to slip planes or normal to slip directions do not contribute to the over-stiffness due to the TFA. Thus, hierarchical multi-laminate (HML) structures are introduced where the successive laminate orientations are taken parallel to the crystal slip planes. It is shown that a conveniently weighted superposition of all the possible plane hierarchies cancels out most of the undesirable TFA contributions to the overall stiffness estimates. A relevant extension to poly-crystal plasticity of this (RSL-TFA-HML) modeling is presented.

Keywords: Microstructures; Crystal plasticity; Elastic-plastic material; Poly-crystalline material; Homogenization

*Corresponding author.

E-mail address: patrick.franciosi@lpmtm.univ-paris13.fr (P. Franciosi).

1. Introduction

Under the rate independence hypothesis, the standard Schmid law (SSL) is the most commonly invoked criterion for crystal plastic flow (Hill and Rice, 1972; Havner, 1973), while power laws are the most widely used for the description of a viscous-plastic slip (Asaro and Needleman, 1985). Yield surfaces resulting from the SSL, multi-potential flow criterion are polyhedrons, the edges and vertices of which correspond to mathematical singularities (Franciosi and Zaoui, 1991). Viscous-plastic modeling provides smoothed yield surfaces, but suffers from other shortcomings, such as, for instance, the coupling with elasticity when used within scale transition methods (Li and Weng, 1997; Sabar et al., 2002; Berbenni et al., 2004).

Meanwhile, a regularized Schmid law (RSL) has been proposed (Arminjon, 1991; Gambin, 1991, 1992; Imbault and Arminjon, 1998) that eliminates the yield surface singularities resulting from the SSL and yet does not require an assumption of time dependence. As a single plastic-potential, microstructure-based model of interest,¹ this RSL has since been extended in different ways to poly-crystals, mostly under the assumptions of either uniform stress or uniform strain (Darrieulat and Piot, 1996; Kowalczyk and Gambin, 2004). Here, we first consider the application of the RSL to heterogeneous intra-crystalline plasticity, because it is now widely admitted that “perfect” crystals also support heterogeneous plastic strains.

Heterogeneous crystal plasticity, although mostly encountered in aggregates where the grains are submitted to multi-axial loading, is a common feature in situations of multi-planar slip when observed at a small enough scale. And, as is now established from Discrete Dislocation Dynamics simulations (Madec et al., 2003), interactions and crossing of dislocations from different planes are less frequent than claimed in forest hardening models (Franciosi, 1985; Kocks et al., 1991; Bassani and Wu, 1991). Increasingly, many heterogeneous models of crystal plasticity attempt to capture similar features, either through the introduction of strain gradients (Fleck et al., 1994; Acharya and Bassani, 2000), or by considering non-local hardening laws (Berveiller et al., 1993; Ortiz et al., 2000), or still by resorting to homogenization (Ponte-Castaneda and Suquet, 1998; Masson et al., 2000). Indeed, heterogeneous behavior strongly suggests treating crystal behavior as an effective one, through an appropriate homogenization scheme. Thus, the extension of the RSL to heterogeneous crystal plasticity proposed herein is performed with reference to a Homogeneous Equivalent Super-Crystal (HESC).

In a second step, we extend the modeling to poly-crystals so as to account for intra and inter granular stress and strain heterogeneities. Because we anticipate plastically homogeneous domains in heterogeneous crystals and in poly-crystals, we propose to use transformation field analysis (TFA) as homogenization procedure (Dvorak, 1992; Dvorak and Benveniste, 1992). The suggested (RSL–TFA) framework is presented in Section 2. The description of the material as an assembly of plastically homogeneous domains is a prerequisite for the TFA procedure to provide correct estimates of the effective material behavior (Suquet, 1997; Chaboche et al., 2001). The TFA is always exact in the limit where each point of the medium is considered a sub-domain. Otherwise, if only the perfect, i.e.

¹When for example implementing crystalline plasticity into finite elements codes devoted to metal forming simulations.

dislocation-free, lattice domains could be considered as plastically homogeneous, the largest validity scale of the TFA would then be the dislocation structure level.

Such perfect lattice domains, corresponding to obstacle-free zones for slip, are well identified by individual orientations in pole figures of single or poly-crystals, and their statistical evolution under load can be quantitatively followed from an analysis of the orientation distribution functions. On the contrary, their morphology in terms of spatial arrangement and individual shapes obeys a complex plasticity-related evolution law which hardly allows for a precise description.

As an attempt to address morphological complexity, we present in Section 3 a simple heterogeneous description of crystal plasticity which formally fulfills the TFA requirement of plastically homogeneous sub-domains. It assumes that, whenever several slip plane orientations are active, slip plane activity is then spatially organized as a multi-laminate structure. The stress and strain fields are known to be almost everywhere uniform in each layer. Many works have been devoted to an analysis of the characteristics and properties of such laminate structures (e.g. Francfort and Murat, 1986; Milton, 1988; Luskin, 1996; Berryman, 2004). Applications to plasticity remain few, for lack of a fully realistic and manageable scheme for microstructure evolution (Ortiz and Repetto, 1999).

The multi-laminate description of intra-crystalline plasticity set up here goes beyond the validation of the proposed (RSL-TFA) framework. It opens applications to poly-crystals. As a first result, we demonstrate the existence of a specific direction of lamination for which the corresponding contributions to the over-stiffness due to the TFA cancel out. We then consider “hierarchical multi-laminate” (HML) structures for slip organization. These are structures made of successive heterogeneity levels of differently oriented rank one-laminates, the orientation at each level being such that the related over-stiffness vanishes. It is then shown that, for an appropriately weighted superposition of the different HML structures that are realizable for a given slip system set, most of the material over-stiffness as estimated from the TFA framework can cancel out.

We finally propose an extension to poly-crystals of this (RSL-TFA-HML) plasticity model that provides correct overall stiffness estimates. As defined, the proposed modeling can be seen as an explicit example, in the case of (poly-) crystal plasticity, of the coupled Non-uniform TFA (NTFA) procedure formally introduced in Michel and Suquet (2003, 2004) for non-linear elastic-plastic heterogeneous solids. In the present work we treat laminates as infinitely flat spheroids. Domain (or grain) edges and corners are not taken into account (e.g. Sarma et al., 2002). Calculations are performed within the commonly used “small strain/large rotation” formalism. We do not incorporate specific features of finite strains (e.g. Fish and Shek, 1999) since those are not expected to influence our main theoretical results. Stiffness comparisons are reported upon in Section 4.

2. The transformation field analysis in a regularized Schmid law for super-crystals

We call “super-crystal” any real or virtual homogeneous structure of volume V where plastic straining results from slip on N^T systems (g) defined by a pair of orthogonal unit vectors \mathbf{n}^g and \mathbf{m}^g , respectively normal to the slip plane and parallel to the slip direction. For each slip system (g) we introduce the Schmid tensor $\tilde{\mathbf{R}}^g = \{\mathbf{m}^g \otimes \mathbf{n}^g\}$, where “ $\{\mathbf{a} \otimes \mathbf{b}\}$ ” (resp. “ $\{\mathbf{a} \otimes \mathbf{b}\}^s$ ”) denotes the “symmetric (resp. skew symmetric) part of $\mathbf{a} \otimes \mathbf{b}$ ”. The discussion is limited to the case where all the slip systems are identical and therefore to the

case where all the slip planes support a same (p)-set of coplanar systems. When real, a super-crystal is a perfect and plastically homogeneous crystal with N slip systems and $P = N/p$ slip planes. The reader may find it useful to think of the octahedral slip in a FCC lattice, where $P = 4$ and $p = 3$, as an illustration.

When virtual, a super-crystal is a homogeneous equivalent medium representing a real heterogeneous (macro-homogeneous) structure of poly-crystalline nature. Those include imperfect crystals, i.e. crystals that contain lattice disorientations which are either grown (mosaic) or to plastic strain-due. Therefore, such a HESC superimposes all the slip systems $g(I)$ that belong to any homogeneous domain (I) of the considered structure, as illustrated in Fig. 1.

2.1. The transformation field analysis (TFA) for heterogeneous crystal plasticity

For any slip system (g) in a super-crystal of volume V , we set $\tau^g(\mathbf{r}) = \mathbf{n}^g \underline{\underline{\boldsymbol{\sigma}}}(\mathbf{r}) \mathbf{m}^g = \underline{\underline{\mathbf{R}}}^g : \underline{\underline{\boldsymbol{\sigma}}}(\mathbf{r}) \geq 0$. It is the currently applied resolved shear stress (ARSS) at any point \mathbf{r} in V . From the affine approximation of Masson et al. (2000) for the homogenization of non-linear heterogeneous materials with local behavior, the stress tensor $\underline{\underline{\boldsymbol{\sigma}}}(\mathbf{r}) = f(\underline{\underline{\boldsymbol{\varepsilon}}}(\mathbf{r}))$ at \mathbf{r} reads as

$$\underline{\underline{\boldsymbol{\sigma}}}(\mathbf{r}) = \underline{\underline{\boldsymbol{\sigma}}}_0(\mathbf{r}) + \left(f(\underline{\underline{\boldsymbol{\varepsilon}}}_0(\mathbf{r})), \underline{\underline{\boldsymbol{\varepsilon}}} \right) : \left(\underline{\underline{\boldsymbol{\varepsilon}}}(\mathbf{r}) - \underline{\underline{\boldsymbol{\varepsilon}}}_0(\mathbf{r}) \right) = \underline{\underline{\mathbf{L}}}_0(\underline{\underline{\boldsymbol{\varepsilon}}}(\mathbf{r})) : \left(\underline{\underline{\boldsymbol{\varepsilon}}}(\mathbf{r}) - \underline{\underline{\boldsymbol{\varepsilon}}}_0^*(\mathbf{r}) \right). \quad (1)$$

Eq. (1), where $f(x_0)$, $x = \partial f(x)/\partial x|_{x_0}$, is the behavior law of a linear comparison material at \mathbf{r} , with the current local tangent moduli $\underline{\underline{\mathbf{L}}}_0(\underline{\underline{\boldsymbol{\varepsilon}}}(\mathbf{r})) = (f(\underline{\underline{\boldsymbol{\varepsilon}}}_0(\mathbf{r})), \underline{\underline{\boldsymbol{\varepsilon}}})$, and with eigenstrains $\underline{\underline{\boldsymbol{\varepsilon}}}_0^*(\mathbf{r}) = \underline{\underline{\boldsymbol{\varepsilon}}}_0(\mathbf{r}) - \underline{\underline{\mathbf{L}}}_0(\underline{\underline{\boldsymbol{\varepsilon}}}(\mathbf{r}))^{-1} : \underline{\underline{\boldsymbol{\sigma}}}_0(\mathbf{r})$. From the standpoint of the time iteration, the problem is then formally the same as that of a thermo-elastic heterogeneous material (Levin, 1967), with an additional iterative adjustment for the current tangent moduli of the ‘‘phases’’ (i.e. the sets of points \mathbf{r} in V which are currently in the same state).

The resulting local stress tensor formally reads as $\underline{\underline{\boldsymbol{\sigma}}}(\mathbf{r}) = \underline{\underline{\mathbf{B}}}_{L_0}(\mathbf{r}) : \underline{\underline{\boldsymbol{\Sigma}}} + \underline{\underline{\boldsymbol{\sigma}}}_{L_0}^{\text{res}}(\mathbf{r})$, where the macroscopic stress tensor $\underline{\underline{\boldsymbol{\Sigma}}}$ is the average stress $\underline{\underline{\boldsymbol{\sigma}}}$, where the stress localization

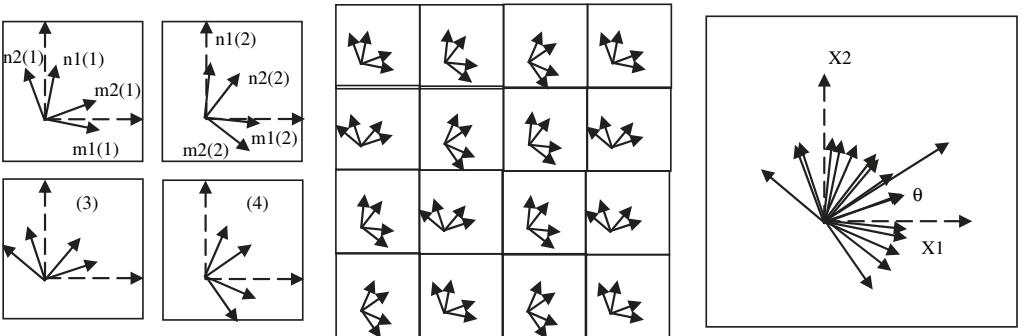


Fig. 1. From left to right, a set of four, differently oriented, homogeneous crystals, a poly-(or multi-) crystalline assemblage, the Homogeneous Equivalent Super-Crystal (HESC).

(or concentration) tensors $\mathbf{B}_{L_0}(\mathbf{r})$ depend on the moduli $\mathbf{L}_0(\underline{\boldsymbol{\varepsilon}}(\mathbf{r}))$, and where the residual stresses $\underline{\boldsymbol{\sigma}}_{L_0}^{\text{res}}(\mathbf{r})$ are obtained from the eigenstrain field as follows:

$$\underline{\boldsymbol{\sigma}}_{L_0}^{\text{res}}(\mathbf{r}) = \int_V \mathbf{F}_{\mathbf{L}_0}(r, r') : \underline{\boldsymbol{\varepsilon}}_0^*(r') \, dr'. \quad (2)$$

The tensors $\mathbf{B}_{L_0}(\mathbf{r})$ and $\mathbf{F}_{L_0}(\mathbf{r}, \mathbf{r}')$ are respectively the stress ‘‘localization’’ and stress ‘‘influence’’ tensors. Their introduction depends on the relevant material morphology. In particular, when the plastic strain field is specified, TFA can be used as a homogenization method (Dvorak and Bahei-El-Din, 1997; Suquet, 1997). The main features of the TFA method (Dvorak, 1992; Dvorak and Benveniste, 1992) are detailed in Appendix A. Since the Hooke elasticity law $\underline{\boldsymbol{\sigma}}(\mathbf{r}) = \mathbf{C}(\mathbf{r}) : (\underline{\boldsymbol{\varepsilon}}(\mathbf{r}) - \underline{\boldsymbol{\varepsilon}}^P(\mathbf{r}))$ is a particular form of Eq. (1), with $\mathbf{C}(\mathbf{r})$ as moduli $\mathbf{L}_0(\underline{\boldsymbol{\varepsilon}}(\mathbf{r}))$, the TFA method can be seen as the affine formulation that uses that elasticity law as linear material of comparison at \mathbf{r} .

With plastic strains $\underline{\boldsymbol{\varepsilon}}^P(\mathbf{r})$ seen as local eigenstrains, the TFA method exactly yields

$$\underline{\boldsymbol{\sigma}}(\mathbf{r}) = \mathbf{B}(\mathbf{r}) : \underline{\boldsymbol{\Sigma}} + \int_V \mathbf{F}(\mathbf{r}, \mathbf{r}') : \underline{\boldsymbol{\varepsilon}}^P(\mathbf{r}') \, dr',$$

where $\mathbf{B}(\mathbf{r}) = \mathbf{B}_{L_0=C}(\mathbf{r})$ and $\mathbf{F}(r, r') = \mathbf{F}_{L_0=C}(r, r')$. In sub-domains $V_I = f_I V$ with uniform elasticity moduli \mathbf{C}^I and homogeneous plastic strains $\underline{\boldsymbol{\varepsilon}}^{PI}$, the average stresses $\underline{\boldsymbol{\sigma}}^I$ thus read as

$$\begin{aligned} \underline{\boldsymbol{\sigma}}^I &= \mathbf{C}^I : (\underline{\boldsymbol{\varepsilon}}^I - \underline{\boldsymbol{\varepsilon}}^{PI}) = \mathbf{B}^I : \underline{\boldsymbol{\Sigma}} + \sum_J \mathbf{F}^{IJ} : \underline{\boldsymbol{\varepsilon}}^{PJ} = \mathbf{B}^I : \underline{\boldsymbol{\Sigma}} + \sum_J (\mathbf{H}^I \delta^{IJ} - f_J \mathbf{L}^{IJ}) : \underline{\boldsymbol{\varepsilon}}^{PJ} \\ &= \mathbf{B}^I : \underline{\boldsymbol{\Sigma}} + \sum_J f_J \mathbf{F}^{IJ} : \underline{\boldsymbol{\varepsilon}}^{PJ}, \end{aligned} \quad (3)$$

where $\underline{\boldsymbol{\varepsilon}}^I$ denotes the related average total strains.² The expressions for the operators \mathbf{H}^I and \mathbf{L}^{IJ} are given in Appendix A. The estimates for the moduli result from a 2-point correlation analysis in the case of an inclusion/matrix structure (Ponte-Castaneda and Willis, 1995) and from a self-consistent approach in the case of aggregates (Hill, 1965). For the aggregates of interest in this study, the TFA method is introduced into the relevant framework. In contrast with the affine formulation, the TFA method does not require a step-wise adjustment of the phase moduli within the already iterative self-consistent scheme. If $\underline{\boldsymbol{\beta}}^P = \underline{\mathbf{E}}^P + \underline{\mathbf{W}}^P$ is the plastic part of the displacement gradient, Levin’s formula (1967) gives as effective plastic strains and plastic rotations the following quantities:

$$\underline{\mathbf{E}}^P = \left\{ \underline{\boldsymbol{\beta}}^P \right\} = \left\{ \sum_I f_I \mathbf{Z}^{II} : \underline{\boldsymbol{\varepsilon}}^{PI} \right\} = \sum_I f_I \mathbf{B}^{II} : \underline{\boldsymbol{\varepsilon}}^{PI}; \quad \underline{\mathbf{W}}^P = \left\} \underline{\boldsymbol{\beta}}^P \right\} = \sum_I f_I \mathbf{U}^{II} : \underline{\boldsymbol{\varepsilon}}^{PI}. \quad (4)$$

²As in Eq. (3), we will use the notation $f_J \underline{\mathbf{Z}}^{JJ} = (\cdot)^{JJ}$ for operators $(\cdot)^{JJ}$ that are proportional to the volume fraction f_J .

As in Eq. (3), the resulting expression for the strains in each phase (I) (Appendix A) then takes the forms:

$$\underline{\underline{\boldsymbol{\varepsilon}}}^I = \underline{\underline{\boldsymbol{\sigma}}}^I + \underline{\underline{\boldsymbol{\varepsilon}}}^{PI} = \underline{\underline{\boldsymbol{A}}}^I : \underline{\underline{\boldsymbol{E}}} + \sum_J \underline{\underline{\boldsymbol{D}}}^{IJ} : \underline{\underline{\boldsymbol{\varepsilon}}}^{PJ} = \underline{\underline{\boldsymbol{A}}}^I : \underline{\underline{\boldsymbol{E}}} + \sum_J f_J \underline{\underline{\boldsymbol{D}}}^{IJ} : \underline{\underline{\boldsymbol{\varepsilon}}}^{PJ}. \quad (5)$$

Eq. (5) introduces the strain influence and strain localization tensors $\underline{\underline{\boldsymbol{D}}}^{IJ} = f_J \underline{\underline{\boldsymbol{D}}}^{IJ}$ and $\underline{\underline{\boldsymbol{A}}}^I$, which are dual to the stress influence and localization tensors $\underline{\underline{\boldsymbol{F}}}^{IJ} = f_J \underline{\underline{\boldsymbol{F}}}^{IJ}$ and $\underline{\underline{\boldsymbol{B}}}^I$. The strain localization tensors $\underline{\underline{\boldsymbol{A}}}^I$ (which depend on the description of the material structure) yield $\underline{\underline{\boldsymbol{B}}}^I = \underline{\underline{\boldsymbol{C}}}^I : \underline{\underline{\boldsymbol{A}}}^I : \underline{\underline{\boldsymbol{S}}}^{\text{eff}}$, where the effective elasticity moduli are given by $\underline{\underline{\boldsymbol{C}}}^{\text{eff}} = \langle \underline{\underline{\boldsymbol{C}}} : \underline{\underline{\boldsymbol{A}}} \rangle = \sum_{I,J} f_I \underline{\underline{\boldsymbol{C}}}^I : \underline{\underline{\boldsymbol{A}}}^J$ and $\underline{\underline{\boldsymbol{S}}}^{\text{eff}} = \langle \underline{\underline{\boldsymbol{S}}} : \underline{\underline{\boldsymbol{B}}} \rangle = (\underline{\underline{\boldsymbol{C}}}^{\text{eff}})^{-1}$. The ARSS $\tau^{g(I)}$ on the system $g(I)$ results from Eq. (3) as³

$$\tau^{g(I)} = \underline{\underline{\boldsymbol{R}}}^{g(I)} : \underline{\underline{\boldsymbol{B}}}^I : \underline{\underline{\boldsymbol{\Sigma}}} + \sum_J \underline{\underline{\boldsymbol{R}}}^{g(I)} : \underline{\underline{\boldsymbol{F}}}^{IJ} : \underline{\underline{\boldsymbol{\varepsilon}}}^{PJ} = \underline{\underline{\boldsymbol{M}}}^{g(I)} : \underline{\underline{\boldsymbol{\Sigma}}} + \sum_J f_J \underline{\underline{\boldsymbol{R}}}^{g(I)} : \underline{\underline{\boldsymbol{F}}}^{IJ} : \underline{\underline{\boldsymbol{\varepsilon}}}^{PJ}. \quad (6)$$

2.2. The TFA framework in the RSL plastic flow criterion

The plastic strain increments in the domains $V_J = f_J V$ are $d\underline{\underline{\boldsymbol{\varepsilon}}}^{PJ} = \sum_{k(J)} \underline{\underline{\boldsymbol{R}}}^{k(J)} d\gamma^{k(J)}$ where $d\gamma^{k(J)}$ is slip increment. With $d\underline{\underline{\boldsymbol{E}}}^P$ from Eq. (4) and $d\underline{\underline{\boldsymbol{E}}}$ the macroscopic total strain increment, the material behavior law becomes:

$$\begin{aligned} d\underline{\underline{\boldsymbol{\Sigma}}} &= \underline{\underline{\boldsymbol{C}}}^{\text{eff}} : d\underline{\underline{\boldsymbol{E}}} - \sum_J \sum_{k(J)=1}^N \left(f_J \underline{\underline{\boldsymbol{B}}}^{k(J)} : \underline{\underline{\boldsymbol{R}}}^{k(J)} d\gamma^{k(J)} \right) \\ &= \underline{\underline{\boldsymbol{C}}}^{\text{eff}} : d\underline{\underline{\boldsymbol{E}}} - \sum_J \sum_{k(J)=1}^N \underline{\underline{\boldsymbol{M}}}^{k(J)} d\bar{\gamma}^{k(J)}. \end{aligned} \quad (7)$$

The treatment of such a heterogeneous medium as a HESC is justified by the similarity of its effective plastic strain increment $d\underline{\underline{\boldsymbol{E}}}^P = \sum_J \sum_{k(J)=1}^N \underline{\underline{\boldsymbol{M}}}^{k(J)} d\bar{\gamma}^{k(J)}$ (written in terms of the mean slip increment $d\bar{\gamma}^{k(J)} = f_J d\gamma^{k(J)}$ over V) with that, given by $d\underline{\underline{\boldsymbol{E}}}^P = \sum_{k=1}^N \underline{\underline{\boldsymbol{R}}}^k d\gamma^k$, for a plastically homogeneous and perfect crystal.

At this point, consider first the SSL as flow criterion. Among the $N_p \subset N^T$ potential slip systems which meet the condition $\max(F^{g(I)}) = \max(\tau^{g(I)} - \tau_c^{g(I)}) = 0$, where $\tau_c^{g(I)}$ is the current critical resolved shear stress (CRSS) for the slip system $g(I)$, the active systems $N_a \subseteq N_p$ are those which also satisfy to $\max(dF^{g(I)}) = \max(d\tau^{g(I)} - d\tau_c^{g(I)}) = 0$. Since plastic strains are treated as “stress-free-strains” in the TFA context, $\underline{\underline{\boldsymbol{\varepsilon}}}^{PJ}, \underline{\underline{\boldsymbol{\Sigma}}} = \mathbf{0}$, so that the various partial derivatives in the expressions for $dF^{g(I)}$ read as

$$\left(\tau^{g(I)}, \underline{\underline{\boldsymbol{\Sigma}}} \right) d\underline{\underline{\boldsymbol{\Sigma}}} = \underline{\underline{\boldsymbol{M}}}^{g(I)} : d\underline{\underline{\boldsymbol{\Sigma}}} = \underline{\underline{\boldsymbol{M}}}^{g(I)} : \underline{\underline{\boldsymbol{C}}}^{\text{eff}} : d\underline{\underline{\boldsymbol{E}}} - \sum_J \sum_{k(J)=1}^N \underline{\underline{\boldsymbol{M}}}^{g(I)} : \underline{\underline{\boldsymbol{C}}}^{\text{eff}} : \underline{\underline{\boldsymbol{M}}}^{k(J)} d\bar{\gamma}^{k(J)}, \quad (8a)$$

³The tensors $\underline{\underline{\boldsymbol{M}}}^{g(I)}$ are (i,j) symmetric by symmetry of $\underline{\underline{\boldsymbol{\Sigma}}}$ and of $\underline{\underline{\boldsymbol{\sigma}}}^I$, since $\underline{\underline{\boldsymbol{R}}}^{g(I)} : \underline{\underline{\boldsymbol{B}}}^I : \underline{\underline{\boldsymbol{\Sigma}}} = \underline{\underline{\boldsymbol{\Sigma}}} : \underline{\underline{\boldsymbol{B}}}^I : \underline{\underline{\boldsymbol{R}}}^{g(I)}$.

$$(\tau_c^{g(I)} - \tau_c^{g(I)}), \bar{\gamma}^{k(J)} = \underline{\Phi}^{g(I)k(J)} + \underset{\sim}{\mathbf{R}}^{g(I)} : \underset{\sim}{\mathbf{F}}^{IJ} : \underset{\sim}{\mathbf{R}}^{k(J)} + \underline{\phi}^{g(I)k(J)} - \underline{h}^{g(I)k(J)} = -\underline{H}_\Sigma^{g(I)k(J)}. \quad (8b)$$

In Eq. (8b), $\underline{\phi}^{g(I)k(J)} = (\underset{\sim}{\mathbf{R}}^{g(I)}, \bar{\gamma}^{k(J)}) : \underset{\sim}{\boldsymbol{\sigma}}^I$, $\underline{\Phi}^{g(I)k(J)} = \underset{\sim}{\mathbf{R}}^{g(I)} : (\underset{\sim}{\mathbf{B}}^I, \bar{\gamma}^{k(J)}) : \underset{\sim}{\boldsymbol{\Sigma}} + \underset{\sim}{\mathbf{R}}^{g(I)} : \sum_L f_L(\underline{\mathbf{F}}^{IL}, \bar{\gamma}^{k(J)}) : \underset{\sim}{\boldsymbol{\varepsilon}}^{PL}$, while the physical hardening matrix $[h]$ results from an evolution law for the CRSS $\tau_c^{g(I)}$ of the form:

$$d\tau_c^{g(I)} = \sum_J \sum_{k(J)}^N h^{g(I)k(J)} d\bar{\gamma}^{k(J)} = \sum_J \sum_{k(J)}^N \underline{h}^{g(I)k(J)} d\bar{\gamma}^{k(J)}. \quad (9)$$

For $J \neq I$, the moduli $h^{g(I)k(J)}$ correspond to the non-local hardening contributions if any. But even in the case when the matrices $[h]$, $[\phi]$ and $[\Phi]$ only contain local terms (i.e., $J = I$), neither $[H_\Sigma]$ nor its dual $[H_E] = [H_\Sigma + \underset{\sim}{\mathbf{M}} : \underset{\sim}{\mathbf{C}}^{\text{eff}} : \underset{\sim}{\mathbf{M}}]$ are local (for a prescribed incremental stress and strain tensor) because of the presence of the matrix $[\underset{\sim}{\mathbf{R}} : \underset{\sim}{\mathbf{F}} : \underset{\sim}{\mathbf{R}}]$.

Now take the RSL as flow criterion. In this case, the plastic flow condition involves a single ‘‘plastic potential’’ F and takes the form:

$$F = \left(\sum_I f_I \sum_{g(I)=1}^N \left(\frac{\tau_c^{g(I)}}{\tau_c^{g(I)}} \right)^n \right)^{1/n} - 1 \tau_{c \text{ ref}} = (F0) \tau_{c \text{ ref}} = 0, \quad (10)$$

where $\tau_{c \text{ ref}}$ is some ‘‘reference’’ critical shear stress. In the following, implicit summations for $g(I)$ or g are to be taken over the N slip systems of the crystalline domains (I). For any domain $V_I = f_I V$ one can write $d\tilde{\boldsymbol{\varepsilon}}^{PI} = f_I d\tilde{\boldsymbol{\varepsilon}}^{PI} = \sum_{g(I)} \underset{\sim}{\mathbf{R}}^{g(I)} d\bar{\gamma}^{g(I)}$ over V . Thus, in the flow condition $dF0 = (F0, \underset{\sim}{\boldsymbol{\Sigma}}) d\underset{\sim}{\boldsymbol{\Sigma}} + \sum_J \sum_{k(J)} (F0, \bar{\gamma}^{k(J)}) d\bar{\gamma}^{k(J)} = 0$, one has

$$\begin{aligned} F0, \underset{\sim}{\boldsymbol{\Sigma}} &= \sum_I \sum_{g(I)} f_I \left(\frac{\tau_c^{g(I)}}{\tau_c^{g(I)}} \right)^{n-1} \frac{\underset{\sim}{\mathbf{M}}^{g(I)}}{\tau_c^{g(I)}} = \sum_I \sum_{g(I)} f_I P0^{g(I)} \underset{\sim}{\mathbf{M}}^{g(I)} \\ &= \sum_I \sum_{g(I)} \bar{P}0^{g(I)} \underset{\sim}{\mathbf{M}}^{g(I)} = \underset{\sim}{\mathbf{N}} 0, \end{aligned} \quad (11a)$$

$$F0, \bar{\gamma}^{k(J)} = \sum_I \sum_{g(I)} f_I \left(\frac{\tau_c^{g(I)}}{\tau_c^{g(I)}} \right)^{n-1} \left(\frac{\tau_c^{g(I)}}{\tau_c^{g(I)}}, \bar{\gamma}^{k(J)} \right) = - \sum_I \sum_{g(I)} \bar{P}0^{g(I)} \tilde{\underline{H}}_\Sigma^{g(I)k(J)}, \quad (11b)$$

with⁴

$$\tilde{\underline{H}}_\Sigma^{g(I)k(J)} = \left(\underline{h}^{g(I)k(J)} \left(\frac{\tau_c^{g(I)}}{\tau_c^{g(I)}} \right) - \underline{\phi}^{g(I)k(J)} \right) - \left(\underset{\sim}{\mathbf{R}}^{g(I)} : \underset{\sim}{\mathbf{F}}^{IJ} : \underset{\sim}{\mathbf{R}}^{k(J)} + \underline{\Phi}^{g(I)k(J)} \right).$$

Since $d\tilde{\boldsymbol{\varepsilon}}^P = (F0, \underset{\sim}{\boldsymbol{\Sigma}}) \tau_{c \text{ ref}} d\lambda = (F0, \underset{\sim}{\boldsymbol{\Sigma}}) d\lambda 0 = \underset{\sim}{\mathbf{N}} 0 d\lambda 0 = \underset{\sim}{\mathbf{N}} d\lambda$, the related mean slip increments over V become

$$d\bar{\gamma}^{k(J)} = (F, \tau^{k(J)}) d\lambda = (F0, \tau^{k(J)}) d\lambda 0 = f_J P0^{k(J)} d\lambda 0 = \bar{P}0^{k(J)} d\lambda 0. \quad (12)$$

⁴The difference between $[\tilde{\underline{H}}_\Sigma]$ and $[\underline{H}_\Sigma]$ is not significant since $(\tau_c^{g(I)}/\tau_c^{g(I)})^n \ll 1$ for weakly active systems.

Consequently, the unique incremental plastic multiplier $d\lambda$ can be expressed as

$$d\lambda = \left(\sum_I f_I \sum_{k(I)} \left(d\bar{\gamma}^{k(I)} \left(\frac{\tau_c^{k(I)}}{\tau_{c \text{ ref}}} \right)^{n/(n-1)} \right)^{(n-1)/n} = \frac{d\lambda_0}{\tau_{c \text{ ref}}}. \quad (13)$$

It corresponds to $d\lambda_0 = (\mathbf{N} \mathbf{0} : d\tilde{\Sigma}) / (H0_\Sigma)$ for a stress load and to $d\lambda_0 = (\mathbf{N} \mathbf{0} : \mathbf{C}^{\text{eff}} : d\tilde{\mathbf{E}}^T) / (H0_E)$ for a strain load.

The hardening modulus $H0_\Sigma$ (resp. $H0_E$) for the HESC thus satisfies

$$\begin{aligned} H0_\Sigma (d\lambda_0)^2 &= H_\Sigma (d\lambda)^2 = \sum_I \sum_{g(I)} \sum_J \sum_{k(J)} \bar{P}0^{g(I)} \tilde{H}_\Sigma^{g(I)k(J)} \bar{P}0^{k(J)} (d\lambda_0)^2 \\ &= \sum_{I,J} \sum_{g(I),k(J)} \tilde{H}_\Sigma^{g(I)k(J)} d\bar{\gamma}^{k(J)} d\bar{\gamma}^{g(I)}, \end{aligned} \quad (14a)$$

$$\begin{aligned} H0_E (d\lambda_0)^2 &= H_E (d\lambda)^2 = \left(H0_\Sigma + \mathbf{N} \mathbf{0} : \mathbf{C}^{\text{eff}} : \mathbf{N} \mathbf{0} \right) (d\lambda_0)^2 \\ &= \sum_{I,J} \sum_{g(I),k(J)} \tilde{H}_E^{g(I)k(J)} d\bar{\gamma}^{k(J)} d\bar{\gamma}^{g(I)}, \end{aligned} \quad (14b)$$

with $\tilde{H}_E^{g(I)k(J)} = \tilde{H}_\Sigma^{g(I)k(J)} + \mathbf{M}^{g(I)} : \mathbf{C}^{\text{eff}} : \mathbf{M}^{k(J)}$. The tangent plastic compliance tensor of the HESC finally becomes

$$d\tilde{\mathbf{E}}^P = \sum_I \sum_{g(I)} \mathbf{M}^{g(I)} d\bar{\gamma}^{g(I)} = \mathbf{N} \mathbf{0} d\lambda_0 = \left(\frac{\mathbf{N} \mathbf{0} \otimes \mathbf{N} \mathbf{0}}{H0_\Sigma} \right) : d\tilde{\Sigma} = \tilde{\mathbf{L}}^P : d\tilde{\Sigma}, \quad (15)$$

with

$$\tilde{\mathbf{L}}^P = (H0_\Sigma)^{-1} \sum_{I,J} \sum_{g(I),k(J)} \left(\bar{P}0^{g(I)} \left(\mathbf{M}^{g(I)} \otimes \mathbf{M}^{k(J)} \right) \bar{P}0^{k(J)} \right).$$

The decomposition of the moduli $\tilde{H}_\Sigma^{g(I)k(J)}$ (see Eq. (11b)) yields the decomposition $H0_\Sigma = H0^{(h,\phi)} + H0^{(\text{RFR},\phi)}$ in Eqs. (14), where $H0^{(\text{RFR},\phi)} \approx H0^{(\text{RFR})}$ and

$$\begin{aligned} H0^{(\text{RFR})} &= - \sum_{I,J} \sum_{g(I),k(J)} \bar{P}0^{g(I)} \left(\mathbf{R}^{g(I)} : \mathbf{F}^{IJ} : \mathbf{R}^{k(J)} \right) \bar{P}0^{k(J)} \\ &= - \sum_{I,J} \sum_{g(I),k(J)} \left(\bar{P}0^{g(I)} \left(\mathbf{R}^{g(I)} \otimes \mathbf{R}^{k(J)} \right) \bar{P}0^{k(J)} \right) :: \mathbf{F}^{IJ}. \end{aligned} \quad (16)$$

The larger the $H0_\Sigma$, the stiffer is the material response to loading. Eq. (16) expresses the over-stiffness resulting from the TFA framework for the HESC of a heterogeneous crystalline material. Note that, here, $H0^{\text{TFA}} = H0^{(\text{RFR},\phi)} \approx H0^{(\text{RFR})}$.

2.3. Application to perfect crystals, disoriented crystals and aggregates

2.3.1. The ideally perfect and homogeneous crystal

A perfect—i.e. mosaic-free and plastically homogeneous—crystalline domain V corresponds to sub-domains (I) that are identical in terms of their Schmid tensors $\tilde{\mathbf{R}}^g$, their

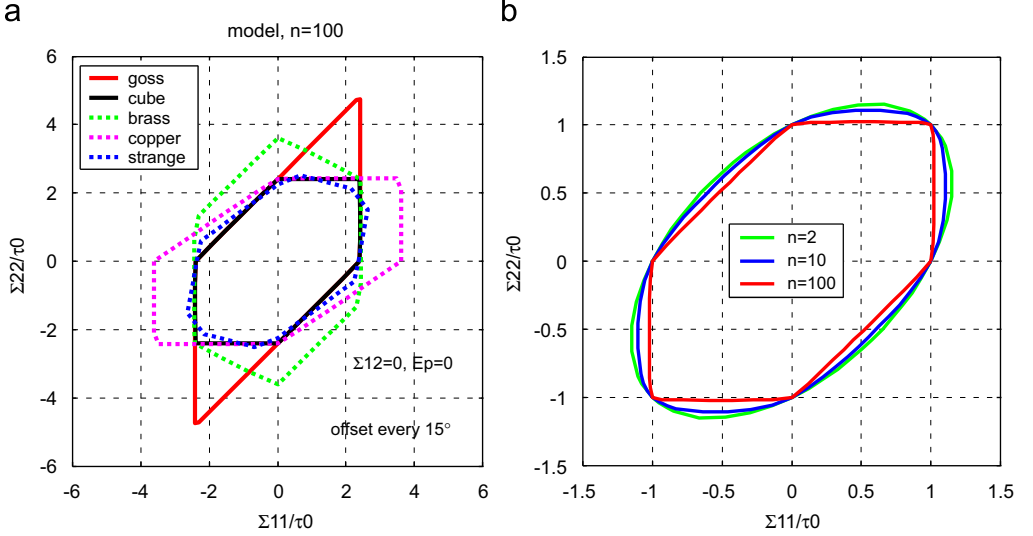


Fig. 2. Yield loci obtained from the RSL-TFA modeling: (a) single crystals of orientation goss $\{110\}\langle 001\rangle$, cube $\{100\}\langle 001\rangle$, brass $\{110\}\langle -112\rangle$, copper $\{112\}\langle 11-1\rangle$, strange $\{123\}\langle 63-4\rangle$; (b) isotropic aggregate of spherical grains.

elasticity moduli \mathbb{C} (such that $\mathbb{A}^I = \mathbb{B}^I = \mathbb{I} \forall I$) and in terms of their slip activity which yields $\mathbb{F} = \mathbf{0}$. This amounts to removing all summations over I in Eq. (10). The model then reduces, as expected, to the classical RSL form for crystals, that is

$$F = \left(\sum_{g=1,N} \left(\frac{\tau^g}{\tau_c} \right)^n - 1 \right) \tau_{c \text{ ref}} = (F0)\tau_{c \text{ ref}} = 0. \quad (17)$$

Sections of yield surfaces for homogeneous crystals are obtained using Eq. (17) as flow criterion. Typical ones are shown in Darrieulat and Piot (1996), or in Kowalczyk and Gambin (2004). A few examples that validate the (RSL-TFA) modeling in this setting for which (RSL-TFA) \equiv (RSL), are shown in Fig. 2(a) reprinted from Berbenni and Franciosi (2004). The selected FCC crystal orientations are typical of ideal FCC texture types and the cubic elasticity anisotropy of aluminium crystals has been used.⁵

The only cause for stiffness evolution in such perfect crystals is the contribution $H0^{(h,\phi)}$ of physical hardening in the equivalent hardening modulus $H0_\Sigma$, and it mostly comes from the matrix $[h]$ that enters the hardening law in Eq. (9). Many tentative descriptions for the physical hardening in crystals can be found in the literature; they will not be commented upon herein (see e.g. Madec et al., 2003; Kocks et al., 1991; Franciosi, 1985, 1988; Estevez et al., 1997). Any description of a local and anisotropic hardening requires at least a pair of hardening moduli ($h0, h$), so as to distinguish “weak” and “strong” slip interactions, with the “reference” modulus ($h0$) and the anisotropy “amplitude” ($a = h/h0 > 1$) varying

⁵ $C_{11} = 114.5$ GPa, $C_{12} = 42.9$ GPa, $C_{44} = 28.6$ GPa.

independently. Assuming isotropic hardening and neglecting rotation (i.e. $h^{gk} = h\mathbf{0}$, $\tau_c^g = \tau_c$ and $[\phi] = 0$, $\forall g, k \in (1, N)$) yields

$$\begin{aligned} H_\Sigma &= \tau_{c \text{ ref}}^2 H\mathbf{0}_\Sigma = h\mathbf{0} \sum_{k=1}^N \sum_{g=1}^N \left(\frac{\tau^g}{\tau_c}\right)^n \left(\frac{\tau_{c \text{ ref}}}{\tau_c}\right)^2 \left(\frac{\tau^k}{\tau_c}\right)^{n-1} \\ &= h\mathbf{0} \left(\frac{\tau_{c \text{ ref}}}{\tau_c}\right)^2 \sum_{k=1}^N \left(\frac{\tau^k}{\tau_c}\right)^{n-1} \cong h\mathbf{0}, \end{aligned} \quad (18)$$

since $n \cong n - 1 \gg 1$. In general, relevant crystal hardening laws are anisotropic, non-linear, and non-convex, as recalled in Section 4.

Now, regardless of the form of $[h]$, the experimentally accessible matrix is $[H_\Sigma]$ (or $[H_E]$). Since $[H_\Sigma]$ only reduces to $[h - \phi]$ (resp. $[H_E]$ to $[h - \phi + \mathbf{R} : \mathbf{C} : \mathbf{R}]$) for vanishing summations over I, J , measurements of the effective hardening $[H_\Sigma]$ (or $[H_E]$) will only provide correct physical hardening estimates for crystals with truly homogeneous behavior.

2.3.2. The disoriented heterogeneous crystal and the aggregate extension

When an imperfect and/or heterogeneous crystal V is treated as perfect and homogeneous, the (RSL-TFA) criterion proposed in Eq. (10) significantly differs from the RSL criterion of Eq. (17). For sub-domains $V_I = f_I V$ treated as homogeneous crystals, the ARSS τ^g and CRSS τ_c^g in Eq. (17) must be understood as average values $\bar{\tau}^g$ and $\bar{\tau}_c^g$ over V , and the RSL for such a structure would be of the form

$$F = \left(\sum_{g=1}^N \left(\frac{\sum_I f_I \tau^{g(I)}}{\sum_I f_I \tau_c^{g(I)}} \right)^n \right)^{1/n} - 1 \tau_{c \text{ ref}} = (F\mathbf{0})\tau_{c \text{ ref}} = 0. \quad (19)$$

The comparison of Eq. (10) with Eq. (19) clearly identifies Eq. (10) as the relevant extension of Eq. (17) to a HESC that represents either an imperfect crystal or a polycrystal. Fig. 2(b) reports the (RSL-TFA) simulation of a yield surface section for an isotropic aggregate of spherical domains (grains or sub-grains) for different values of n . The related section of the yield surface from the SSL matches that of the RSL for $n \gg 1$.

A plot of (normalized) axial versus tangential stresses is compared in Fig. 3 with that of a re-crystallized aluminium polycrystal obtained from experimental texture data in Althoff and Wincierz (1972). This simulation is obtained from an idealized texture fitted to the experimental one by using six appropriately weighted ideal orientations (Fig. 4). The use of a normal Gaussian distribution of 100 orientations around each ideal orientation provides 2400 grain orientations by orthotropic symmetry (Bunge, 1982). As a comparison, for that same texture, Fig. 3 also reports the Taylor–Bishop–Hill estimate which assumes plastic strain uniformity (Bishop and Hill, 1951). As expected in the self-consistent framework, the results with the (RSL-TFA) modeling are closer to the experimental results than those with the Taylor–Bishop–Hill modeling.

The above arguments demonstrate that the (RSL-TFA) modeling is convenient for determining aggregate yield surfaces, whether or not the description of the plastic field heterogeneities is fully consistent from the standpoint of the TFA. The improvement of the modeling of crystalline plasticity with regard to this consistency is addressed below.

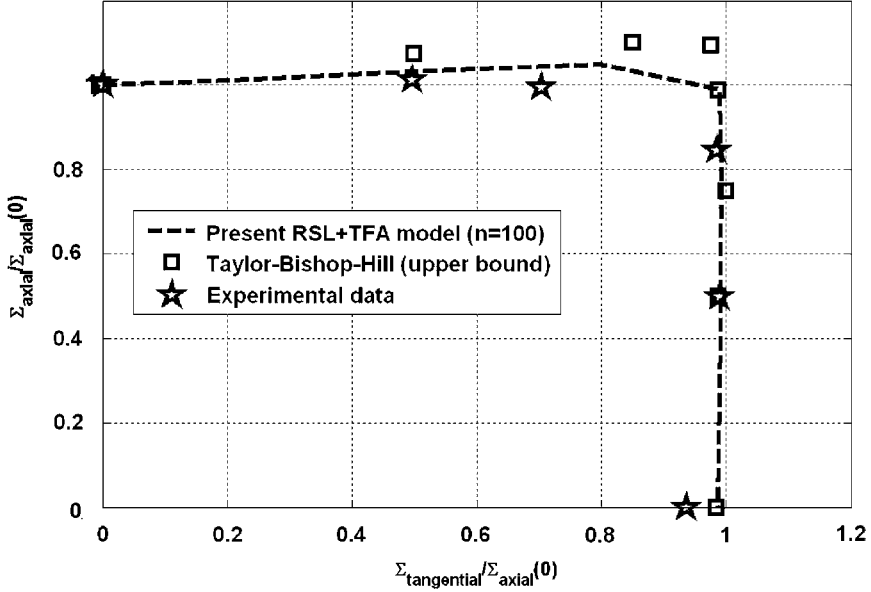


Fig. 3. Yield loci of recrystallized Al: comparison between the (RSL-TFA) modeling (dashed line), the Taylor–Bishop–Hill upper bound (squares) and data (pentagrams) from Althoff and Wincierz (1972).

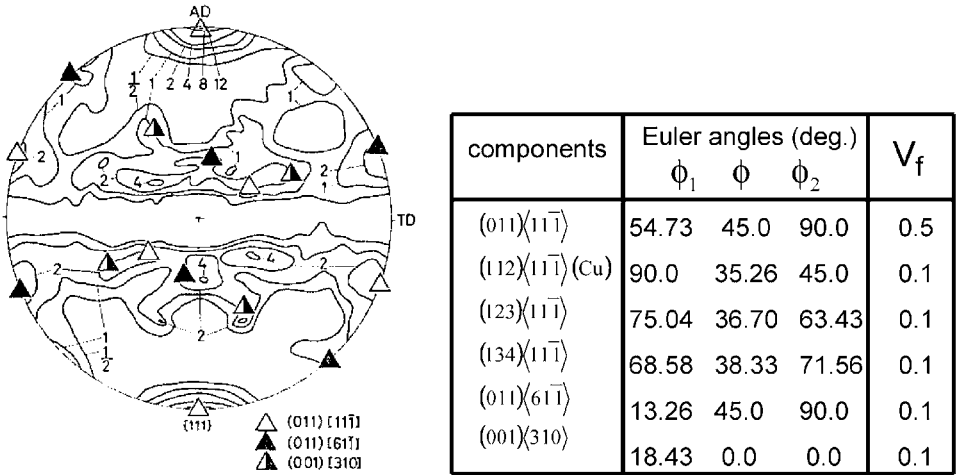


Fig. 4. The considered experimental texture (the $\{111\}$ pole figure from Althoff and Wincierz, 1972) and its idealized orientation distribution function described by their Euler angles used in Fig. 3.

2.3.3. Effective (overall) versus crystal (local) hardening

For disoriented crystals as for aggregates, even the simplest local isotropic physical hardening law in crystalline homogeneous sub-domains (I) corresponds, when non-linear, to different current CRSS τ_c^I and to different reference moduli h_0^I . This is because they exhibit different plastic strain states. The extended RSL enables us to consider various

possible descriptions of crystal hardening in terms of the local and non-local contributions in $[h]$ in Eq. (9). Interactions of non-local nature between sub-domain pairs (I - J) may lead to disorientation effects (Mecif et al., 1997) or to strain gradient effects (Acharya and Bassani, 2000) resulting from the spatial organization of slip. The latter is controlled by the form of the allowed paths through the dislocation arrays. However, a hardening model should not depend on a particular choice of homogenization framework, and variations on $[h]$ will not be addressed here.

Aside from $[h]$, the ‘‘accommodation effects’’ in $[H_\Sigma] = [(h - \phi) - (\Phi + \mathbf{R} : \underline{\mathbf{F}} : \mathbf{R})]$ result from the operators $\underline{\mathbf{F}}$ and from the matrix $[\Phi]$. If comparing the inhomogeneous case with its homogeneous analogue, the effective material stiffness $H0_\Sigma$ in the RSL now differs from the actual stiffness $H0^{(h,\phi)}$ because of the additional contribution $H0^{(\text{RFR},\Phi)} \approx H0^{(\text{RFR})}$ in Eq. (16) that is mainly because of the terms $[\mathbf{R} : \underline{\mathbf{F}} : \mathbf{R}]$ in $[H_\Sigma] \approx [h - \mathbf{R} : \underline{\mathbf{F}} : \mathbf{R}]$. Because of the influence operators $\underline{\mathbf{F}}$ whose terms are of the same magnitude as the material elasticity moduli, the TFA is expected to result—for a fixed morphology—in the largest and most substantial difference between effective and physical hardening. It is through a maximal reduction of the difference ($[H_\Sigma] - [h]$), or $(H0_\Sigma - H0^{(h,\phi)})$ that one can hope to ensure the constraint of plastic homogeneity in the various sub-domains and thus validate the use of the TFA.

Consequently, a good description of heterogeneous intra-crystalline plasticity must satisfy $[H_\Sigma] \approx [h]$, i.e. $H0^{(\text{RFR},\Phi)} \approx H0^{(\text{RFR})} \ll H0^{(h,\phi)}$. Section 3 further comments on this, prior to presenting a description which formally fulfills the TFA request of plastically homogeneous sub-domains. The proposed description significantly reduces the value $H0^{\text{TFA}} \approx H0^{(\text{RFR})}$ compare to that of $H0^{(h,\phi)}$ for heterogeneous crystals and for polycrystals.

3. Heterogeneous descriptions of intra-crystalline plasticity in the RSL-TFA framework

We introduce a heterogeneous description of crystal plasticity considering a self-organization of multi-laminate nature for the slip activity. We point first at some specific characteristics of intra-crystalline partitions into homogeneous sub-domains.

3.1. General features of the RSL-TFA framework for heterogeneous intra-crystalline plasticity

Heterogeneous crystals which may exhibit sub-domains with different slip patterns can be considered in a two-level extension of the (RSL)-(TFA) criterion of Eq. (10) of the form:

$$F = \left(\sum_I f_I \left[\sum_{\alpha(I)} f_{\alpha(I)} \sum_{g(\alpha(I))} \left(\frac{\tau_c^{g(\alpha(I))}}{\tau_c} \right)^n \right] \right)^{1/n} - 1 \Big|_{\tau_{\text{c ref}}} = 0. \quad (20)$$

Eq. (20) has different possible meanings. The contribution sets $\alpha(I)$, related to a grain type (I), can be seen either as sub-domains occupying volume fractions $f_{\alpha(I)}$, or as different possible flow solutions with occurrence probabilities $f_{\alpha(I)}$, or also as sub-groups of the N

slip systems (as for example the coplanar systems), to which possible different activity “weights”, or volume fractions, $f_{\alpha(I)}$ are assigned.

Under the first two assumptions, the number of the contribution sets $\alpha(I)$ in a grain is freely defined while the number of the terms $g(\alpha(I))$ inside each set $\alpha(I)$ is the slip system number N . In that respect, the elementary sub-domains are crystal-like. Under the third assumption of P sub-groups of slip systems, $\alpha(I) \in (1, P)$, $g(\alpha(I)) \in (1, p = N/P)$, and the elementary sets $\alpha(I)$ are sets of “crystal-unlike” domains in the sense that all the N slip systems are not identically able to activate in them. However, regardless of the interpretation given to Eq. (20) and of the related morphology description, the consideration of two heterogeneity levels in the (RSL-TFA) framework amounts to modifying the stress localization and influence operators $\underline{\mathbf{B}}^I$ and $\underline{\mathbf{F}}^{IJ}$ in the ARSS $\tau^{g(I)}$ of Eq. (6), as well as the related strain operators.

In the now heterogeneous domains (I), one has the effective stress $\underline{\boldsymbol{\sigma}}^I = \underline{\mathbf{B}}^I : \underline{\boldsymbol{\Sigma}} + \sum_{Jf} f \underline{\mathbf{F}}^{IJ} : \underline{\boldsymbol{\varepsilon}}^{PJ} = \underline{\mathbf{B}}^I : \underline{\boldsymbol{\Sigma}} + \sum_J \underline{\mathbf{F}}^{IJ} : \underline{\boldsymbol{\varepsilon}}^{PJ}$, where $\underline{\boldsymbol{\varepsilon}}^{PJ} = \sum_{\beta(J)} f_{\beta(J)} \underline{\mathbf{B}}^{I\beta(J)} : \underline{\boldsymbol{\varepsilon}}^{P\beta(J)}$ is the effective plastic strain for the domain (J). This yields, in the sub-domain $\alpha(I)$:

$$\begin{aligned} \underline{\boldsymbol{\sigma}}^{\alpha(I)} &= \underline{\mathbf{B}}^{\alpha(I)} : \left(\underline{\mathbf{B}}^I : \underline{\boldsymbol{\Sigma}} + \sum_J \underline{\mathbf{F}}^{IJ} : \underline{\boldsymbol{\varepsilon}}^{PJ} \right) + \sum_{\beta(I)} \underline{\mathbf{F}}^{\alpha(I)\beta(I)} : \underline{\boldsymbol{\varepsilon}}^{P\beta(I)} \\ &= \underline{\mathbf{B}}^{\alpha I} : \underline{\boldsymbol{\Sigma}} + \sum_{\beta_J} \underline{\mathbf{F}}^{\alpha I \beta_J} : \underline{\boldsymbol{\varepsilon}}^{P\beta_J} = \underline{\boldsymbol{\sigma}}^{\alpha I}. \end{aligned} \quad (21a)$$

The operators $\underline{\mathbf{B}}^{\alpha I}$ and $\underline{\mathbf{F}}^{\alpha I \beta_J}$ which substitute for the operators $\underline{\mathbf{B}}^I$ and $\underline{\mathbf{F}}^{IJ}$ of Eqs. (3) and (6) read as

$$\underline{\mathbf{B}}^{\alpha I} = \underline{\mathbf{B}}^{\alpha(I)} : \underline{\mathbf{B}}^I, \quad \underline{\mathbf{F}}^{\alpha I \beta_J} = \frac{1}{f_{\beta_J}} \underline{\mathbf{F}}^{\alpha I \beta_J} = \underline{\mathbf{B}}^{\alpha(I)} : \underline{\mathbf{F}}^{IJ} : \underline{\mathbf{B}}^{I\beta(J)} + \frac{\delta^{IJ}}{f_J} \underline{\mathbf{F}}^{\alpha(I)\beta(I)}, \quad f_{\beta_J} = f_{Jf} f_{\beta(J)}. \quad (21b)$$

For elastically and plastically homogeneous grains, one has $\underline{\mathbf{B}}^{\alpha(I)} = \underline{\mathbf{A}}^{\alpha(I)} = \underline{\mathbf{I}}, \forall \alpha(I)$, and $\underline{\mathbf{F}}^{\alpha(I)\beta(I)} = \underline{\mathbf{D}}^{\alpha(I)\beta(I)} = \underline{\mathbf{0}}, \forall (\alpha(I), \beta(I))$. Heterogeneous crystal plasticity with null or neglected lattice disorientations corresponds to $\underline{\mathbf{F}}^{\alpha(I)\beta(I)} \neq \underline{\mathbf{0}}$ and $\underline{\mathbf{D}}^{\alpha(I)\beta(I)} \neq \underline{\mathbf{0}}$, still with $\underline{\mathbf{B}}^{\alpha(I)} = \underline{\mathbf{A}}^{\alpha(I)} = \underline{\mathbf{I}}$.

A partition of each “phase” (I) into a number P of sub-domains where all the N slip systems can operate will thus yield a (NP) set of operators $\underline{\mathbf{B}}^{\alpha(I)}$ and a $(NP \times NP)$ matrix of operators $[\underline{\mathbf{F}}^{\alpha(I)\beta(I)}]$. A “crystal-unlike” partition into P identical sub-groups of $p = N/P$ identical slip systems as the coplanar system sets will accordingly correspond to a (pP) set of operators $\underline{\mathbf{B}}^{\alpha(I)}$ made of P sub-groups of p identical operators, and to a $(pP \times pP)$ matrix of operators $[\underline{\mathbf{F}}^{\alpha(I)\beta(I)}]$ made of $P \times P$ blocs of $p \times p$ identical operators, as illustrated in

Eqs. (22) for $P = 4$ and $p = 3$:

$$\left(\underset{\approx}{\mathbf{B}}^{\alpha(I)} \right) = \left(\left(\underset{\approx}{\mathbf{B}}^{1(I)}, \underset{\approx}{\mathbf{B}}^{1(I)}, \underset{\approx}{\mathbf{B}}^{1(I)} \right), \left(\cdot, \underset{\approx}{\mathbf{B}}^{2(I)}, \cdot \right), \left(\cdot, \underset{\approx}{\mathbf{B}}^{3(I)}, \cdot \right), \left(\cdot, \underset{\approx}{\mathbf{B}}^{4(I)}, \cdot \right) \right), \quad (22a)$$

$$\left[\underset{\approx}{\mathbf{F}}^{z(I)\beta(I)} \right] = \left[\begin{array}{ccc} \left[\begin{array}{ccc} \underset{\approx}{\mathbf{F}}^{1(I)1(I)} & \underset{\approx}{\mathbf{F}}^{1(I)1(I)} & \underset{\approx}{\mathbf{F}}^{1(I)1(I)} \\ \underset{\approx}{\mathbf{F}}^{1(I)1(I)} & \underset{\approx}{\mathbf{F}}^{1(I)1(I)} & \underset{\approx}{\mathbf{F}}^{1(I)1(I)} \\ \underset{\approx}{\mathbf{F}}^{1(I)1(I)} & \underset{\approx}{\mathbf{F}}^{1(I)1(I)} & \underset{\approx}{\mathbf{F}}^{1(I)1(I)} \end{array} \right] & \left[\begin{array}{c} \underset{\approx}{\mathbf{F}}^{1(I)2(I)} \\ \cdot \\ \cdot \end{array} \right] & \left[\begin{array}{c} \underset{\approx}{\mathbf{F}}^{1(I)3(I)} \\ \cdot \\ \cdot \end{array} \right] & \left[\begin{array}{c} \underset{\approx}{\mathbf{F}}^{1(I)4(I)} \\ \cdot \\ \cdot \end{array} \right] \\ \left[\begin{array}{c} \cdot \\ \underset{\approx}{\mathbf{F}}^{2(I)1(I)} \\ \cdot \end{array} \right] & \left[\begin{array}{c} \underset{\approx}{\mathbf{F}}^{2(I)2(I)} \\ \cdot \\ \cdot \end{array} \right] & \left[\begin{array}{c} \cdot \\ \cdot \\ \cdot \end{array} \right] & \left[\begin{array}{c} \cdot \\ \cdot \\ \cdot \end{array} \right] \\ \left[\begin{array}{c} \cdot \\ \underset{\approx}{\mathbf{F}}^{3(I)1(I)} \\ \cdot \end{array} \right] & \left[\begin{array}{c} \cdot \\ \cdot \\ \cdot \end{array} \right] & \left[\begin{array}{c} \cdot \\ \cdot \\ \cdot \end{array} \right] & \left[\begin{array}{c} \cdot \\ \cdot \\ \cdot \end{array} \right] \\ \left[\begin{array}{c} \cdot \\ \cdot \\ \cdot \end{array} \right] & \left[\begin{array}{c} \cdot \\ \cdot \\ \cdot \end{array} \right] & \left[\begin{array}{c} \cdot \\ \cdot \\ \cdot \end{array} \right] & \left[\begin{array}{c} \cdot \\ \cdot \\ \cdot \end{array} \right] \end{array} \right]. \quad (22b)$$

From Eq. (20), the overall hardening modulus $H0_{\Sigma}$ for the HESC is obtained by writing:

$$H0_{\Sigma}(\mathrm{d}\lambda 0)^2 = \sum_I \sum_J \sum_{\alpha(I)} \sum_{\beta(J)} \sum_{g(\alpha(I))} \sum_{k(\beta(J))} \tilde{\mathbf{H}}_{\Sigma}^{g(\alpha(I))k(\beta(J))} \mathrm{d}\bar{\gamma}^{k(\beta(J))} \mathrm{d}\bar{\gamma}^{g(\alpha(I))}. \quad (23)$$

In the effective hardening matrix $[\tilde{\mathbf{H}}_{\Sigma}]$ of Eq. (23), as in Eqs. (14), no particular choice of physical hardening model can compensate for the contributions from the matrix $[\mathbf{R} : \underset{\approx}{\mathbf{F}} : \mathbf{R}]$. From now on, in order to formally ensure the TFA request of plastically homogeneous sub-domains, we take HML structures to be the typical intra-crystalline organizations of multi-planar slip (Franciosi and Berbenni, 2005, 2006). We first present the HML structures that we consider in this study and we next examine them with regard to resulting overall stiffness.

3.2. A hierarchical multi-laminate (HML) structure for intra-crystalline plastic slip

The investigated HML structures for intra-crystalline slip can be described as follows.

(i) *Description of a HML intra-crystalline slip organization:* The plastic strain is taken as homogeneous in any domain where a single slip plane orientation (A) is currently active. A second active slip plane orientation (B) is assumed to form a two-phase rank-one laminate structure with (A), denoted $A|B$. Similarly, a third slip plane orientation (C) is assumed to form a second level of two-phase rank-one laminate structure with the homogeneous equivalent medium (AB) of level one. This results in a rank-two laminate structure denoted by $AB|C = A|B|C$. Successive laminations are thus repeated up to the last slip plane orientation (P). Thus, P plane orientations form $(P-1)$ -HML structures of rank $(P-1)$. For FCC crystals, $P = 4$ yields (3)-HML structures $A|B|C|D$. As described, the laminations are domains of incremental coplanar slip.

During each increment, a first “natural” assumption is that the successive laminations are parallel to the different slip plane orientations, although, for compatibility reasons,

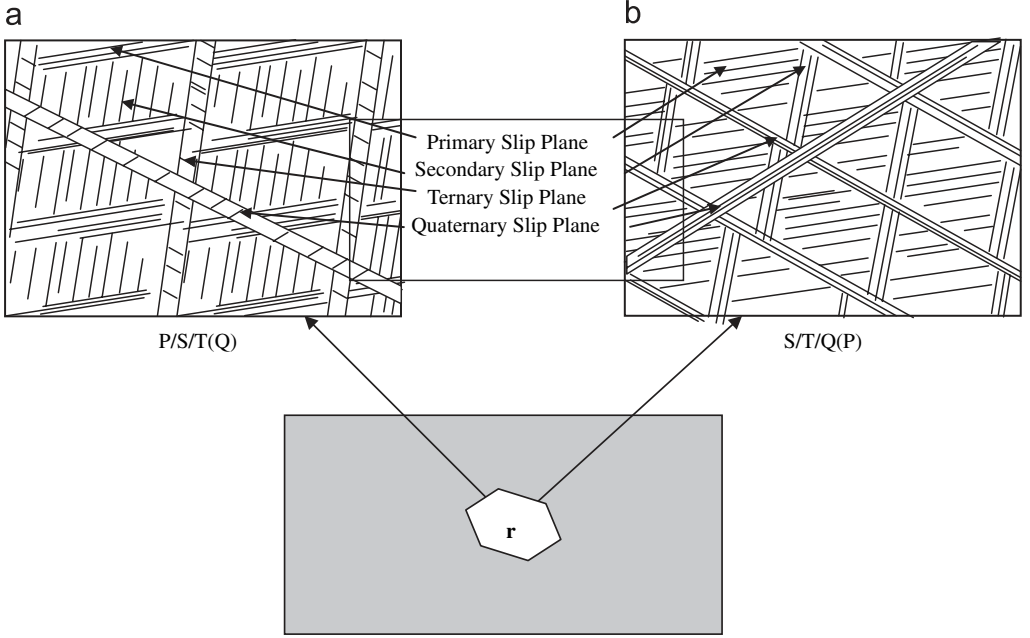


Fig. 5. Scheme of an intra-crystalline (3)—HML structure for (a) the $P/S/T(Q)$ and (b) the $S/T/Q(P)$ slip plane hierarchy occurring at any point r in (c) the whole HESC, with $p(a)$ and $p(b)$ probabilities.

other orientations may be preferred, as Ortiz and Repetto (1999) thoroughly examined in the case of FCC crystals. Another “natural” assumption is to choose the first laminate orientation (A) parallel to the Primary—i.e. most active—slip plane type (P), the secondary laminate orientation (B) parallel to the Secondary active slip plane type (S), etc. When $P = 4$, this yields the $P|S|T|(Q)$ hierarchy (with “ T ” for “Ternary” and “ Q ” for “Quaternary” active slip plane type), as illustrated in Fig. 5(a).

This lamination hierarchy can be expected to be generally the dominant one. However, situations where several slip plane hierarchies are equivalent call for some weighted superposition of the different hierarchy possibilities (i.e. the number $P!$ of the slip plane permutations) in terms of the respective occurrence probabilities.

We denote by $I|J|K|\dots|(P)$ the hierarchy where the slip plane (I) defines the primary laminate orientation (A) but is not necessarily the Primary active slip plane type, where the slip plane (J) defines the secondary laminate orientation (B) but is not necessarily the Secondary active slip plane type, and so on. As an example, Fig. 5(b) displays for $P = 4$ the hierarchy $S|T|Q|(P)$. The occurrence probability $p^{(I|J|K|\dots|(P))}$ for the $I|J|K|\dots|(P)$ hierarchy can be expressed as

$$\begin{aligned}
 p^{(I|J|K|\dots|(P))} &= p(P - 1 / \dots / K / J / I) \\
 &= p(I) \left(\frac{p(J)}{1 - p(I)} \right) \left(\frac{p(K)}{1 - (p(I) + p(J))} \right) \dots = \prod_{U=1}^{P-1} \frac{p(U)}{1 - \sum_{V=1}^{U-1} p(V)},
 \end{aligned} \tag{24a}$$

where $p(I)$ denotes the probability that plane (I) defines the primary laminate orientation (A), $p(J/I) = p(I)p(J)/(1 - p(I))$ stands for the conditional probability for plane (J) to define the secondary laminate orientation (B) when plane (I) defines the primary one, etc.

Thus, at any point \mathbf{r} of V as illustrated in Fig. 5(c), each of the possible HML structures ($h \in (1, P!)$) for slip organization can be found with probability $p^{(h)}$, the mean solution for the plastic flow in V being obtained from their statistical average. In so doing, although each individual HML organization yields a heterogeneous solution (h), the mean solution can be considered as statistically uniform in the HESC. Finally, the probabilities $p(I)$ can be connected to the relative incremental slip activities on the planes (I). We here define them as

$$p(I) = \frac{\sum_{g(I)} d\gamma^{g(I)}}{\sum_I \sum_{g(I)} d\gamma^{g(I)}} = \frac{\sum_{g(I)} P0^{g(I)}}{\sum_I \sum_{g(I)} P0^{g(I)}}. \quad (24b)$$

These evolving probabilities account for incremental evolutions of the HML structures, in terms of the plastic strain (and rotation) evolutions, even though the structures keep a constant ($P-1$) rank.

(ii) *Constitutive equations for the HML organization of intra-crystalline slip:* The successive load increments are applied to the incrementally updated HESC. In the level-1 laminate structure $A|(B)$, “phase” (B) is taken as the matrix phase, while “phase” (C) is consecutively taken as the matrix phase in the level-2 laminate structure $A|B|(C)$, etc. At each successive homogenization level, the newly added matrix phase can have a different (differently oriented) elasticity tensor. Since all k -levels are two-phase laminates $\Omega|(M)$, all summations or mean values $\langle \cdot \rangle$ involve only two terms $J_k = (\Omega, M)$ at each level (k). This yields the exact influence tensor at each level, and consequently yields an exact and unique overall such tensor for each HML structure. The recurrent connection between the successive levels ($\dots, k-1, k, k+1, \dots$) is that (omitting I) the average stress increment $\langle d\tilde{\boldsymbol{\sigma}}_{k-1} \rangle$ at level ($k-1$) defines that, $d\tilde{\boldsymbol{\sigma}}_k^\Omega$, of the included phase at level (k). Thus, with $\langle d\tilde{\boldsymbol{\sigma}}_{P-1} \rangle = d\tilde{\boldsymbol{\Sigma}}$, the stress increments of the phases (J_k) at level (k), read as, for $k \in (1, P-1)$

$$\begin{aligned} d\tilde{\boldsymbol{\sigma}}_k^J &= \underset{\approx}{\mathbf{B}}_k^J : \left(\underset{\approx}{\mathbf{B}}_{k+1}^\Omega : \left(\dots : \left(\underset{\approx}{\mathbf{B}}_{P-1}^\Omega : d\tilde{\boldsymbol{\Sigma}} + \sum_{J'_{P-1}} f_{J'}^{(P-1)} \underset{\approx}{\mathbf{F}}_{P-1}^{\Omega J'} : d\tilde{\boldsymbol{\varepsilon}}_{P-1}^{PJ'} \right) + \dots \right) \right. \\ &\quad \left. + \sum_{J'_{k+1}} f_{J'}^{(k+1)} \underset{\approx}{\mathbf{F}}_{k+1}^{\Omega J'} : d\tilde{\boldsymbol{\varepsilon}}_{k+1}^{PJ'} \right) + \sum_{J'_k} f_{J'}^{(k)} \underset{\approx}{\mathbf{F}}_k^{\Omega J'} : d\tilde{\boldsymbol{\varepsilon}}_k^{PJ'}. \end{aligned} \quad (25a)$$

The P plastically homogeneous phases being the ($P-1$) matrix phases M_k , $k \in (1, P-1)$, plus the included phase Ω_1 at the first laminate level, one can write the intermediate effective plastic strain increments as

$$\begin{aligned} d\tilde{\boldsymbol{\varepsilon}}_{k+1}^{PJ} &= \sum_{J_k} f_{J_k}^{(k)} \underset{\approx}{\mathbf{B}}_k^{tJ} : \left(d\tilde{\boldsymbol{\varepsilon}}_k^{PJ} \right) = f_\Omega^{(k)} \underset{\approx}{\mathbf{B}}_k^{t\Omega} : \left(d\tilde{\boldsymbol{\varepsilon}}_k^{PJ} \right) + f_M^{(k)} \underset{\approx}{\mathbf{B}}_k^{tM} : d\tilde{\boldsymbol{\varepsilon}}_k^{PM} \\ &= f_\Omega^{(k)} \underset{\approx}{\mathbf{B}}_k^{t\Omega} : \left(\dots : \left(f_\Omega^{(2)} \underset{\approx}{\mathbf{B}}_2^{t\Omega} \left(f_\Omega^{(1)} \underset{\approx}{\mathbf{B}}_1^{t\Omega} : d\tilde{\boldsymbol{\varepsilon}}_1^{P\Omega} + f_M^{(1)} \underset{\approx}{\mathbf{B}}_1^{tM} : d\tilde{\boldsymbol{\varepsilon}}_1^{PM} \right) \right. \right. \\ &\quad \left. \left. + f_M^{(2)} \underset{\approx}{\mathbf{B}}_2^{tM} : d\tilde{\boldsymbol{\varepsilon}}_2^{PM} \right) + \dots \right) + f_M^{(k)} \underset{\approx}{\mathbf{B}}_k^{tM} : d\tilde{\boldsymbol{\varepsilon}}_k^{PM}. \end{aligned} \quad (25b)$$

Eqs. (25a, b) finally provide, for the plastically homogeneous “phases” $\pi, \pi' \in (1, P)$, the operators $\underline{\underline{\mathbf{B}}}^\pi$ and $\underline{\underline{\mathbf{F}}}^{\pi\pi'}$ which characterize the $(P-1)$ -HML structure presented here. These operators relate the phase stress increments to the phase (homogeneous) plastic strain increments according to

$$d\tilde{\underline{\underline{\sigma}}}^\pi = \underline{\underline{\mathbf{B}}}^\pi : d\tilde{\underline{\underline{\Sigma}}} + \sum_{\pi'} f_{\pi'} \underline{\underline{\mathbf{F}}}^{\pi\pi'} : d\tilde{\underline{\underline{\varepsilon}}}^{P\pi'} \quad (26)$$

The operator sets $(\underline{\underline{\mathbf{B}}}^\pi, \underline{\underline{\mathbf{F}}}^{\pi\pi'})$, $\pi, \pi' \in (1, P)$, are a special case of the operator sets $(\underline{\underline{\mathbf{B}}}^{\alpha(I)}, \underline{\underline{\mathbf{F}}}^{\alpha(I)\beta(I)})$ for a grain or a crystal-like sub-domain (I) in Eqs. (21). They are given in Appendix B when $P = 4$ for general lamination volume fractions f_π . From Eqs. (25a, b), the localization operators $\underline{\underline{\mathbf{B}}}^\pi$ are products $(\underline{\underline{\mathbf{B}}}^1 : \dots : \underline{\underline{\mathbf{B}}}^P : \underline{\underline{\mathbf{B}}}^K)$ of similar operators over k successive lamination levels $(1 \leq k \leq P-1)$. Accordingly, the influence operators $\underline{\underline{\mathbf{F}}}^{\pi\pi'}$ are $(P-1)$ -sums of mixed products $(\underline{\underline{\mathbf{B}}}^1 : \dots : \underline{\underline{\mathbf{B}}}^K : (\underline{\underline{\mathbf{F}}}^{K\lambda}) : \underline{\underline{\mathbf{B}}}^{l\lambda} : \dots : \underline{\underline{\mathbf{B}}}^{l\phi})$, each mixed product involving a single elementary influence operator $\underline{\underline{\mathbf{F}}}^{K\lambda}$ that corresponds to that of the k levels of the $(P-1)$ -HML structure. The operators $\underline{\underline{\mathbf{F}}}^{\pi\pi'}$ of Eq. (26) will be examined in the next section. Some key properties are first established under the assumption of preserved homogeneous elasticity in the material (i.e. $\underline{\underline{\mathbf{B}}}^\pi = \underline{\underline{\mathbf{I}}}$, $\forall \pi \in I$). They are next shown to be valid for aggregates of heterogeneous elasticity as well.

3.3. The particular characteristics of the considered HML structures

3.3.1. The form of the operators $\underline{\underline{\mathbf{F}}}^{\pi\pi'}$ for HML structures

From Eq. (26)—neglecting the terms $[\phi]$ and $[\Phi]$ given in Eq. (8b)—one can express the ARSS increment on the slip system $g(\pi)$ of the domain π as

$$d\tau^{g(\pi)} = \underline{\underline{\mathbf{R}}}^{g(\pi)} : d\tilde{\underline{\underline{\sigma}}}^\pi = \underline{\underline{\mathbf{R}}}^{g(\pi)} : \underline{\underline{\mathbf{B}}}^\pi : d\tilde{\underline{\underline{\Sigma}}} + \sum_{\pi'} \sum_{k(\pi')} f_{\pi'} \left(\underline{\underline{\mathbf{R}}}^{g(\pi)} : \underline{\underline{\mathbf{F}}}^{\pi\pi'} : \underline{\underline{\mathbf{R}}}^{k(\pi')} \right) d\gamma^{k(\pi')}. \quad (27)$$

Eq. (27) is valid regardless of the number of slip systems (whether it be one, a coplanar set, or all) that are considered in each domain π . Now, in any $(P-1)$ -HML structure $A|B|C|\dots|(P)$, the set of influence tensors, which contribute to the terms $[\underline{\underline{\mathbf{R}}} : \underline{\underline{\mathbf{F}}} : \underline{\underline{\mathbf{R}}}]$, corresponds (Appendix B) to a set of “stress” Green operator integrals $\underline{\underline{\mathbf{t}}}_{C\pi}^{\prime\pi}$, $\pi = A, B, C, \dots, P-1$ which are characteristic of the platelet-like laminate layers $A, B, C, \dots, P-1$. Given slip-plane-oriented laminates, the resulting specific properties are

- (i) A single platelet operator up to rotation for a given slip plane type: each platelet operator $\underline{\underline{\mathbf{t}}}_{C\pi}^{\prime\pi}$ depends on the elasticity moduli $\underline{\underline{\mathbf{C}}}^\pi$ of the matrix phase in the π -oriented layers. But the lattice is identically oriented in all the platelet local frames when all platelets are parallel to slip planes of a same type (like $(1\ 1\ 1)$ planes in a FCC lattice). Therefore, all the platelet operators involved are identical, up to a rotation, and can be denoted $\underline{\underline{\mathbf{t}}}_{C\pi}^{\prime\pi}$.

- (ii) Platelet operator of isotropic-like elasticity: as long as one can assume isotropic elasticity in the slip planes, the expression of the reference platelet operator is similar to that for fully isotropic elasticity, say $t_{pqjn}^P = a\delta_{pqjn}^A(\omega) + b\delta_{pqjn}^B(\omega)$, with $\delta_{pqjn}^A(\omega) = \omega_j\omega_p\omega_n\omega_q$, $\delta_{pqjn}^B(\omega) = (\Delta_{jp}\omega_n\omega_q)|_{(p,q),(j,n)}$ and where $\omega_1 = \sin\theta\cos\phi$, $\omega_2 = \sin\theta\sin\phi$, $\omega_3 = \cos\theta$ (Franciosi and Lormand, 2004), but with appropriate (a, b) coefficient values.⁶ Thus, in the platelet frame, the platelet strain Green operator $\underline{\underline{\mathbf{t}}}^\pi$ and its dual stress operator $\underline{\underline{\mathbf{t}}}^\pi = \underline{\underline{\mathbf{C}}} - \underline{\underline{\mathbf{C}}} : \underline{\underline{\mathbf{t}}}^\pi : \underline{\underline{\mathbf{C}}}$ which appears in the tensors $\underline{\underline{\mathbf{F}}}$ (Appendix A) take the non-zero forms reported in Table 1 (for $\omega^\pi//x_3$ when $\theta = 0$, and using the 6×6 contracted matrix notation for the rank-four tensors in R^3).
- (iii) ‘‘Orthogonality’’ property of platelet operators with Schmid tensors: in a slip-plane-oriented laminate π , the Schmid tensors $\underline{\underline{\mathbf{R}}}^{g(\pi)}$ for all coplanar systems in (π) take the related vector form $(0, 0, 0, R_{23}^{g(\pi)}, R_{31}^{g(\pi)}, 0)$ in the laminate frame where $\mathbf{n}^{g(\pi)} = (0, 0, 1)$ and $\mathbf{m}^{g(\pi)} = (m_1^{g(\pi)}, m_2^{g(\pi)}, 0)$. Consequently, $\underline{\underline{\mathbf{R}}}^{g(\pi)} : \underline{\underline{\mathbf{t}}}^\pi = 0$ and no product of the form $\underline{\underline{\mathbf{R}}}^{g(\pi)} : \underline{\underline{\mathbf{t}}}^\pi : \underline{\underline{\mathbf{R}}}^{k(\pi')}$ or $\underline{\underline{\mathbf{R}}}^{g(\pi)} : \underline{\underline{\mathbf{t}}}^{\pi'} : \underline{\underline{\mathbf{R}}}^{k(\pi')}$ contributes to the terms $\underline{\underline{\mathbf{R}}}^{g(\pi)} : \underline{\underline{\mathbf{F}}}^{\pi\pi'} : \underline{\underline{\mathbf{R}}}^{k(\pi')}$ characterizing the HML structure from Eq. (27), i.e. in the $H0^{(\text{RFR}, \Phi)} = H0^{\text{TFA}}$ terms of Eq. (16). For $P = 4$, the expression of these terms when the elasticity is homogeneous ($\underline{\underline{\mathbf{B}}}^\pi = \underline{\underline{\mathbf{I}}}$) can be obtained from Table 2 which fully reports, in that case, the matrix of the stress influence operators $\underline{\underline{\mathbf{F}}}^{\pi\pi'} = f_{\pi'}\underline{\underline{\mathbf{F}}}^{\pi\pi'}$. It is noteworthy that slip systems having their slip direction normal to a laminate plane (i.e. $\mathbf{m}^{g(\pi)} = (0, 0, 1)$, $\mathbf{n}^{g(\pi)} = (n_1^{g(\pi)}, n_2^{g(\pi)}, 0)$) also do not contribute to the part $H0^{\text{TFA}}$ of the overall stiffness modulus;
- (iv) Linear decomposition of the influence tensors into elementary operators: thanks to the previous considerations, all the influence tensors $\underline{\underline{\mathbf{F}}}^{\pi\pi'} = f_{\pi'}\underline{\underline{\mathbf{F}}}^{\pi\pi'}$ of any $(P-1)$ -HML structure $A|B|C|\dots|(P)$ finally rearrange into linear combinations of the same set of slip-plane-oriented platelet operators $(\underline{\underline{\mathbf{t}}}^A, \underline{\underline{\mathbf{t}}}^B, \underline{\underline{\mathbf{t}}}^C, \dots)$ so that $\underline{\underline{\mathbf{F}}}^{\pi\pi'} = \sum_{\pi''} \phi_{\pi''}^{\pi\pi'} \underline{\underline{\mathbf{t}}}^{\pi''}$. The last plane type (P) never contributes. But all the P plane types participate in turn since all the $(P!)$ plane permutations are taken into account with appropriate probabilities. In this expression for $\underline{\underline{\mathbf{F}}}^{\pi\pi'}$, not every coefficient $\phi_{\pi''}^{\pi\pi'}$ is positive, owing to the dependency relations between the influence tensors that yield

$$\begin{aligned} \sum_{\pi'=1,P} \phi_{\pi''}^{\pi\pi'} &= 0, \quad \forall \pi \in (1, P), \quad \forall \pi'' \in (1, P-1), \\ \sum_{\pi=1,P} f_{\pi} \phi_{\pi''}^{\pi\pi'} &= 0, \quad \forall \pi' \in (1, P), \quad \forall \pi'' \in (1, P-1). \end{aligned} \quad (28)$$

- (v) Generalization to heterogeneous elasticity: as far as elasticity heterogeneities due solely to rotations are concerned, as is the case for heterogeneous crystals and

⁶ (a, b) depends on the crystallographic type of the laminate plane and on the elasticity anisotropy of the considered crystal.

Table 1

The non zero parts of the dual platelet operators \mathbf{t}^P and \mathbf{t}'^P , as viewed from the platelet frame

\mathbf{t}	11	22	33	23	31	12
11						
22						
33			t_{33}	t_{34}	t_{35}	
23			t_{34}	t_{44}	t_{45}	
31			t_{35}	t_{45}	t_{55}	
12						
\mathbf{t}'	11	22	33	23	31	12
11	t'_{11}	t'_{12}				
22	t'_{12}	t'_{22}				
33						
23						
31						
12						t'_{66}

Table 2

The phase stress influence operators of the TFA, $\mathbf{F}^{\pi\pi'} = f_{\pi} \mathbf{F}^{\pi\pi'} = \sum_{\pi''} \phi_{\pi''}^{\pi\pi'} \mathbf{t}^{\pi''}$ of Eq. (27), for a (3)—HML structure, in the homogeneous elasticity case ($f_{\pi}^3 = 1 - f_{\pi}$, $\pi = A, B, C, D$)

$\begin{bmatrix} -\left(\frac{F_B}{F_A+F_B}\right) \mathbf{t}^A \\ -\left(\frac{F_C}{1-F_D} \frac{F_A}{F_A+F_B}\right) \mathbf{t}^B \\ -\left(F_D \frac{F_A}{1-F_D}\right) \mathbf{t}^C \end{bmatrix}$	$\begin{bmatrix} +\left(\frac{F_B}{F_A+F_B}\right) \mathbf{t}^A \\ -\left(\frac{F_C}{1-F_D} \frac{F_B}{F_A+F_B}\right) \mathbf{t}^B \\ -\left(F_D \frac{F_B}{1-F_D}\right) \mathbf{t}^C \end{bmatrix}$	$\begin{bmatrix} +\left(\frac{F_C}{1-F_D}\right) \mathbf{t}^B \\ -\left(F_D \frac{F_C}{1-F_D}\right) \mathbf{t}^C \end{bmatrix}$	$\begin{bmatrix} +\left(F_D\right) \mathbf{t}^C \end{bmatrix}$
$\begin{bmatrix} +\left(\frac{F_A}{F_A+F_B}\right) \mathbf{t}^A \\ -\left(\frac{F_C}{1-F_D} \frac{F_A}{F_A+F_B}\right) \mathbf{t}^B \\ -\left(F_D \frac{F_A}{1-F_D}\right) \mathbf{t}^C \end{bmatrix}$	$\begin{bmatrix} -\left(\frac{F_A}{F_A+F_B}\right) \mathbf{t}^A \\ -\left(\frac{F_C}{1-F_D} \frac{F_B}{F_A+F_B}\right) \mathbf{t}^B \\ -\left(F_D \frac{F_B}{1-F_D}\right) \mathbf{t}^C \end{bmatrix}$	$\begin{bmatrix} +\left(\frac{F_C}{1-F_D}\right) \mathbf{t}^B \\ -\left(F_D \frac{F_C}{1-F_D}\right) \mathbf{t}^C \end{bmatrix}$	$\begin{bmatrix} +\left(F_D\right) \mathbf{t}^C \end{bmatrix}$
$\begin{bmatrix} +\left(\frac{F_A}{1-F_D}\right) \mathbf{t}^B \\ -\left(F_D \frac{F_A}{1-F_D}\right) \mathbf{t}^C \end{bmatrix}$	$\begin{bmatrix} +\left(\frac{F_B}{1-F_D}\right) \mathbf{t}^B \\ -\left(F_D \frac{F_B}{1-F_D}\right) \mathbf{t}^C \end{bmatrix}$	$\begin{bmatrix} -\left(\frac{F_A+F_B}{1-F_D}\right) \mathbf{t}^B \\ -\left(F_D \frac{F_C}{1-F_D}\right) \mathbf{t}^C \end{bmatrix}$	$\begin{bmatrix} +\left(F_D\right) \mathbf{t}^C \end{bmatrix}$
$\begin{bmatrix} +\left(F_A\right) \mathbf{t}^C \end{bmatrix}$	$\begin{bmatrix} +\left(F_B\right) \mathbf{t}^C \end{bmatrix}$	$\begin{bmatrix} +\left(F_C\right) \mathbf{t}^C \end{bmatrix}$	$\begin{bmatrix} -\left(1-F_D\right) \mathbf{t}^C \end{bmatrix}$

poly-crystals of a single crystalline phase, properties (i) and (ii) are maintained. For property (iii), from the expressions $\mathbf{H}^I = -\mathbf{t}^{iI} : \mathbf{Y}^I : \mathbf{t}^{iI} = \mathbf{H}^{II} = -\mathbf{t}^{iI} : \mathbf{B}^{II} = -\mathbf{B}^I : \mathbf{t}^{iI}$, and $f_J \mathbf{E}^{IJ} = \mathbf{H}^J : (\mathbf{I} \delta^{IJ} - f_J \mathbf{B}^{IJ}) = (\mathbf{I} \delta^{IJ} - f_J \mathbf{B}^J) : \mathbf{H}^J$ for aggregates treated in the self-consistent scheme (Appendix A), all products of the form $\mathbf{R}^{g(\pi)} : (\mathbf{t}^{\pi} : \mathbf{Y} : \mathbf{t}^{\pi'})$ or $(\mathbf{t}^{\pi'} : \mathbf{Y} : \mathbf{t}^{\pi'}) : \mathbf{R}^{k(\pi')}$ also do not contribute to $H0^{\text{RFR}}$ in Eq. (16). One also easily

verifies that $\underset{\approx}{\mathbf{R}}^{g(\pi)} : \underset{\approx}{\mathbf{H}}^\pi = \underset{\approx}{\mathbf{H}}^\pi : \underset{\approx}{\mathbf{R}}^{k(\pi)} = 0$, since, as for $\underset{\approx}{\mathbf{t}}^{\pi'}$ in Table 1, the non-zero H_{ij}^π terms of $\underset{\approx}{\mathbf{H}}^\pi$ are for $(i = 1, 2, 6)$. For property (iv), a linear decomposition of the influence operators still holds but only over the full set of elementary operators $(\underset{\approx}{\mathbf{H}}^\pi, \underset{\approx}{\mathbf{L}}^{\pi\pi'})$, $\pi, \pi' = (A, B, C, \dots)$, with $\underset{\approx}{\mathbf{L}}^{\pi\pi'} = \underset{\approx}{\mathbf{B}}^\pi : \underset{\approx}{\mathbf{H}}^{\pi'} = \underset{\approx}{\mathbf{H}}^\pi : \underset{\approx}{\mathbf{B}}^{\pi'}$.

3.3.2. Material stiffness resulting from the HML organization of intra-crystalline slip

The description of the HML structures reported in Section 3.2 does not specify in detail how the different slip contributions of the π planes, $\pi \in (1, P)$, stepwise interpenetrate each other, or, in other words, how the plastic strain heterogeneity is spatially organized in the material. Nevertheless, each possible slip plane hierarchy $(h) = I|JK| \dots |L)$ among the $P!$ ones that yield a specific coefficient matrix $\phi_{\pi\pi'}^{(h)\pi''}$ is a potential incremental heterogeneous plastic straining “mode”, with evolving occurrence probability $p^{(h)}$ from Eq. (24a).

The statistical average of all these possible HML plastic straining modes provides a mean coefficient matrix $\langle \phi_{\pi\pi'}^{\pi''} \rangle = \sum_{h=1}^{P!} p^{(h)} \phi_{\pi\pi'}^{(h)\pi''}$ for the elementary influence operators $\underset{\approx}{\mathbf{t}}^{\pi''}$. Under the assumption of isotropic elasticity, the terms of the resulting matrix of mean influence operators thus simply read $\langle \underset{\approx}{\mathbf{F}}^{\pi\pi'} \rangle = \sum_{\pi''=1, P} \langle \phi_{\pi\pi'}^{\pi''} \rangle \underset{\approx}{\mathbf{t}}^{\pi''}$. All P slip-plane-oriented platelet operators are involved in that expression through the contributions of all $P!$ plane permutations. Finally, although the individual HML structures have been built assuming spatially separated incremental slip plane activities, the mean solution obtained by superposition of the individual ones can be considered as spatially homogeneous from an ergodicity condition. This superposition also allows us to disregard length-scale and other compatibility restrictions on the multi-laminate structures.

The P -heterogeneous partition of the crystal that results from this (HML) modeling finally corresponds to assuming P sub-domain types whose relative volume fractions are step-wise defined from Eq. (24b) as $f_\pi = p(I = \pi)$, and within which all P slip planes are accounted for. The superposition of the $P!$ different solutions from each possible $(P-1)$ -HML organization of slip amounts to coupling the corresponding $P!$ heterogeneous intra-crystalline plastic strain “modes”. In that respect, the proposed (HML) modeling can be seen as a special case, for crystalline plasticity, of the coupled non-uniform TFA (NTFA) proposed by Michel and Suquet (2003, 2004) for general non-linear elastic-plastic materials. This NTFA has been shown to remove the over-stiffness due to the TFA by a relevant choice of plastic modes, as the (TFA-HML) modeling does here. Thanks to the HML structure attributed to slip, the resulting expression for $H0^{\text{TFA}} \approx H0^{(\text{RFR})}$ from Eq. (16), denoted $H0^{\text{TFA-HML}}$, then reads as

$$\begin{aligned} H0^{\text{TFA-HML}} &= \sum_{\pi''} \sum_{\pi, \pi'} \sum_{g\pi, k\pi'} P0^{g\pi} \underset{\approx}{\mathbf{R}}^{g\pi} : \underset{\approx}{\mathbf{t}}^{\pi''} : \underset{\approx}{\mathbf{R}}^{k\pi'} P0^{k\pi'} \Big) f_\pi \langle \phi_{\pi\pi'}^{\pi''} \rangle \\ &= \sum_{\pi''} \sum_{\pi, \pi'} f_\pi \sum_{g\pi, k\pi'} P0^{g\pi} \underset{\approx}{\mathbf{R}}^{g\pi} \otimes \underset{\approx}{\mathbf{R}}^{k\pi'} P0^{k\pi'} \Big) :: \langle \phi_{\pi\pi'}^{\pi''} \rangle \underset{\approx}{\mathbf{t}}^{\pi''}, \end{aligned} \quad (29)$$

using $\langle \underset{\approx}{\mathbf{F}}^{\pi\pi'} \rangle = f_{\pi'} \langle \underset{\approx}{\mathbf{F}}^{\pi\pi'} \rangle = \sum_{\pi''} \langle \phi_{\pi\pi'}^{\pi''} \rangle \underset{\approx}{\mathbf{t}}^{\pi''}$ according to Appendix B.

Since the mean weight matrix $\langle \phi_{\pi\pi'}^{\pi''} \rangle$ obeys Eq. (28) for all the terms π'' separately, this incremental contribution of the TFA to the crystal stiffness globally vanishes in any symmetric situation where the scalar terms $P0^{g\pi} \tilde{\mathbf{R}}^{g\pi} \otimes \tilde{\mathbf{R}}^{k\pi'} P0^{k\pi'}$ are identical for symmetric sets of planes.

This ‘‘symmetry property’’ is not specific to the HML structures since it does not depend on the type of the influence operator. But, in the present case of (HML) intra-crystalline structures, the stiffness term given by Eq. (29) can globally vanish even in the absence of such a symmetry if all the products of the form $P0^{g\pi} \langle \phi_{\pi\pi'}^{\pi''} \rangle P0^{k\pi'}$ (no summations over repeated indices) where $\pi'' \neq (\pi, \pi')$ are weak enough to have a total negligible contribution to $H0^{\text{TFA-HML}}$. Note that these individual contributions are not zero because of the orthogonality property. This is nearly achieved for the slip planes hierarchies considered here, whose non-vanishing terms dominantly correspond to the slip planes of weak incremental activity. Therefore, when such a HML structure is considered to describe a heterogeneous intra-crystalline plasticity, no or little material over-stiffness comes from the TFA framework.

Consequently, for either an initial mosaic or a strain-induced crystallographic heterogeneity, a homogenization procedure using the (TFA-HML) scheme proves consistent with the assumption that $H0_{\Sigma} \approx H0^{(h,\phi)}$ (i.e. $[H_{\Sigma}] \approx [h]$) when matching $[H_{\Sigma}]$ to experimental crystal hardening. Furthermore, this analysis of intra-crystalline plasticity in terms of HML structures for the slip organization indicates an application method of the (TFA-HML) scheme to polycrystalline structures.

3.4. Application of the (HML) modeling to poly-crystal plasticity description

Let us consider aggregates of homogeneous isotropic elasticity for simplicity sake. The most straightforward extension of the (TFA-HML) scheme to a polycrystal is a direct application of Eq. (29) to its HESC, with a double summation running over all pairs of slip planes of all grains. But such a treatment of all slip planes at the same heterogeneity level results in a total loss of grain shape effects. When conversely preserving the two distinct heterogeneity levels that characterize aggregates of heterogeneous grains, the influence operators from Eqs. (21a) and (21b) enable us to extend $H0^{\text{TFA-HML}}$ from $H0^{(\text{RFR})}$ in Eq. (16) as follows:

$$\begin{aligned} H0^{\text{TFA-HML}} &= \sum_{I,J} \left(\sum_{\alpha(I),\beta(J)} \sum_{g(\alpha(I)),k(\beta(J))} \bar{P}0^{g(\alpha(I))} \left(\tilde{\mathbf{R}}^{g(\alpha(I))} : \underline{\mathbf{F}}^{\alpha I \beta J} : \tilde{\mathbf{R}}^{k(\beta(J))} \right) \bar{P}0^{k(\beta(J))} \right) \\ &= \sum_{I,J} \sum_{\pi(I),\pi'(J)} \sum_{g(\pi(I)),k(\pi'(J))} \left(P0^{g(\pi(I))} \tilde{\mathbf{R}}^{g(\pi(I))} \otimes \tilde{\mathbf{R}}^{k(\pi'(J))} P0^{k(\pi'(J))} \right) \\ &\quad :: \left(f_{I'} f_{\pi(I)} f_{J'} f_{\pi'(J)} \left(\underline{\mathbf{F}}^{IJ} + \frac{\delta^{IJ}}{f_J} \underline{\mathbf{F}}^{\pi(I)\pi'(J)} \right) \right). \end{aligned} \quad (30)$$

The indices (α, β) are changed into (π, π') to represent an intra-crystalline P -partition ‘‘built from’’ the P slip planes of the grain (I) according to the previously defined mean HML structure. Accordingly, $\bar{P}0^{g(\pi(I))} = f_{I'} f_{\pi(I)} P0^{g(\pi(I))} = f_{\pi_I} P0^{g(\pi(I))}$. The intra-granular operators $f_{\pi'(I)} \underline{\mathbf{F}}^{\pi(I)\pi'(I)} = \sum_{\pi'' I} \langle \phi_{\pi'' I}^{\pi I \pi' I} \rangle \mathbf{t}^{\pi'' I}$ which result from the (HML) scheme, as given in Eq. (29), are different $P \times P$ matrices of $\underline{\mathbf{F}}^{\pi(I)\pi'(I)}$ operators for each grain (I).

On the contrary, all grains of an aggregate are described by a unique “shape” operator, generally of ellipsoidal symmetry, \mathbf{t}'^G , in such a way that one obtains $\mathbf{F}^{IJ} = (1 - \delta^{IJ}/f_I)\mathbf{t}'^G$ in Eq. (30), from Eq. (A.10) and from the following ones in Appendix A. The TFA over-stiffness for an aggregate of homogeneous grains then results from the non-vanishing tensor products $(\mathbf{R}^{g(\pi(I))} \otimes \mathbf{R}^{k(\pi'(J))}) :: \mathbf{t}'^G$ that we now examine. Making use of the Inverse Radon transform of the Green operators (Franciosi and Lormand, 2004), one can write $\mathbf{t}'^G = \int_{\Omega} \Psi_{(\omega)}^G \mathbf{t}'^{\omega} d\omega$, which is a continuously weighted linear decomposition of \mathbf{t}'^G on the platelet operators \mathbf{t}'^{ω} of ω -oriented normal in R^3 .

This decomposition, with $d\omega = \sin \theta d\theta d\phi$ running over the Ω unit sphere, and which is such that $\int_{\Omega} \Psi_{(\omega)}^G d\omega = 1$ and $\Psi_{(\omega)}^G \geq 0$, enables us to establish that the tensor products $(\overline{P}0^{g(\pi(I))} \mathbf{R}^{g(\pi(I))} \otimes \mathbf{R}^{k(\pi'(J))} \overline{P}0^{k(\pi'(J))}) :: \mathbf{t}'^G$ partly vanish because of the orthogonality property pointed out in Section 3.3.1. In particular, the contributions involving the platelets that are parallel to slip planes of dominant activity are eliminated, as well as the contributions from platelets that are perpendicular to slip directions. This implies that a relevant extension of the (HML) scheme to poly-crystals consists in part in replacing the continuous decomposition \mathbf{t}'^G by a discrete one $\mathbf{t}'^{(G)}$ which only retains the operators of the platelets oriented parallel to the slip planes in the aggregate, their summation being weighted in a manner such as to take into account both the relative plastic activities of the slip plane types, and the shape effect of the grains. This set could be complemented, if necessary and under conditions that remain to be specified, by the operators of the platelets which are orthogonal to slip directions,⁷ but those are ignored here.

For example, let us take

$$\mathbf{t}'^G \approx \frac{\sum_I f_I \sum_{\pi(I)} f_{\pi(I)} \Psi_{\pi(I)}^G \mathbf{t}'^{\pi(I)}}{\sum_I f_I \sum_{\pi(I)} f_{\pi(I)} \Psi_{\pi(I)}^G},$$

instead of \mathbf{t}'^G in the two-level (HML) scheme defined by Eq. (30). Apart from the effects of relative grain concentrations and of relative slip activities through the f_I and $f_{\pi(I)}$ values, respectively, the grain shape (and shape change) effect is preserved in \mathbf{t}'^G through the retained part $(\Psi_{\pi(I)}^G)$ of the grain shape characteristic function $(\Psi_{(\omega)}^G)$.

When intra-crystalline heterogeneities are disregarded, substituting $\mathbf{t}'^{(G)}$ for \mathbf{t}'^G is also a convenient extension of the TFA-HML approach to polycrystalline aggregates of homogeneous grains. It is noteworthy that such a $\mathbf{t}'^{(G)}$ operator is implicitly representative of some mean HML organization of slip for the poly-crystal or its HESC.

⁷Laminates being plastically homogeneous everywhere except in small layers near their boundaries, the arrangement of these platelets with regard to the slip systems are consistent with low energy dislocation planar arrays as “carpets” and as “walls”, respectively in slip planes and normal to them (Kulhmann-Wilsdorf, 2002).

4. Simulation examples comparing the (TFA) and (TFA-HML) modeling

For simplicity sake, we consider cases of bi-crystalline aggregates with grain volume fractions f_1, f_2 , and with each grain type (I) possibly supporting one initial disorientation (or CRSS heterogeneity) between two types of sub-domains with volume fractions $f_{1(I)}, f_{2(I)}$. Only two non-coplanar slip systems can contribute to the plastic strain in each domain type ($N = P = 2, p = 1$). At most, this corresponds, with reference to Fig. 1, to a four-domain structure involving eight differently active slip planes. That structure will be called the “mosaic bi-crystal” for short. Particular sub-cases are the “bi-crystal” (no sub-domains in the grains), the (single) “mosaic crystal” and the (single) crystal.

The bi-crystal and the mosaic crystal are highly textured aggregates exhibiting only two different lattice orientations. The domains have congruent ellipsoidal shapes and fixed volume fractions for the bi-crystal, while they are of laminate type with slip-dependent volume fractions for mosaic crystals. For each sub-domain $\alpha(I)$, the two ($P! = 2$) permitted (1)-HML structures correspond to laminates that are parallel either to the Primary or to the Secondary slip plane. They correspond to the hierarchies $P|(S)_{\alpha I}$ and $S|(P)_{\alpha I}$, according to previously introduced notation.

Eqs. (24) provides their occurrence probabilities,

$$p(\pi(\alpha I)) = f_{\pi(\alpha I)} = \frac{P0^{\pi(\alpha I)}}{P0^{1(\alpha I)} + P0^{2(\alpha I)}}, \quad \text{for } \pi = (P, S) = (1, 2),$$

and the intra-crystalline influence operators read as $f_{\pi(\alpha I)} \mathbf{F}^{\pi(\alpha I)\pi'(\alpha I)} \approx \sum_{\pi''(\alpha I)} \langle \phi_{\pi''(\alpha I)}^{\pi(\alpha I)\pi'(\alpha I)} \rangle \mathbf{t}_{\approx}^{\pi''(\alpha I)} = (f_{\pi} - \delta_{\pi\pi'})_{\alpha I} \hat{\mathbf{t}}_{\approx}^{\prime(\alpha I)}$, with $\hat{\mathbf{t}}_{\approx}^{\prime(\alpha I)} = f_{1(\alpha I)} \hat{\mathbf{t}}_{\approx}^{\prime 1(\alpha I)} + f_{2(\alpha I)} \hat{\mathbf{t}}_{\approx}^{\prime 2(\alpha I)}$. For spherical domains or sub-domains, one can write $\mathbf{t}_{\approx}^{\prime G} = \mathbf{t}_{\approx}^{\prime \text{SPH}} = (1/4\pi) \int_{\Omega} \mathbf{t}_{\approx}^{\prime \omega} d\omega$. In the HML modeling, the sphere operator $\mathbf{t}_{\approx}^{\prime \text{SPH}}$ will be replaced by $\mathbf{t}_{\approx}^{\prime(\text{SPH})} = \sum_I f_I \sum_{\alpha I} f_{\alpha I} \sum_{\pi(\alpha I)} f_{\pi(\alpha I)} \mathbf{t}_{\approx}^{\prime \pi(\alpha I)}$ for the mosaic bi-crystal. In the bi-crystal case, the summation over α vanishes and $\mathbf{t}_{\approx}^{\prime(\text{SPH})} = \sum_I f_I \sum_{\pi(I)} f_{\pi(I)} \mathbf{t}_{\approx}^{\prime \pi(I)} = \sum_I f_I \hat{\mathbf{t}}_{\approx}^{\prime(I)}$, so that the 4×4 matrix of the (TFA-HML) influence operators $\mathbf{F}_{\approx \text{TFA-HML}}^{\pi I \pi' J} = f_J f_{\pi'(J)} \mathbf{F}_{\approx}^{\pi I \pi' J}$ takes the form

$$\mathbf{F}_{\approx \text{TFA-HML}}^{\pi I \pi' J} = \begin{bmatrix} \begin{bmatrix} -f_{1(1)}f_{2\approx} \mathbf{t}_{\approx}^{\prime(\text{SPH})} & -f_{2(1)}f_{2\approx} \mathbf{t}_{\approx}^{\prime(\text{SPH})} \\ -f_{2(1)} \hat{\mathbf{t}}_{\approx}^{\prime(1)} & +f_{2(1)} \hat{\mathbf{t}}_{\approx}^{\prime(1)} \end{bmatrix} & \begin{bmatrix} f_{1(2)}f_{2\approx} \mathbf{t}_{\approx}^{\prime(\text{SPH})} & f_{2(2)}f_{2\approx} \mathbf{t}_{\approx}^{\prime(\text{SPH})} \\ +0 & +0 \end{bmatrix} \\ \begin{bmatrix} -f_{1(1)}f_{2\approx} \mathbf{t}_{\approx}^{\prime(\text{SPH})} & -f_{2(1)}f_{2\approx} \mathbf{t}_{\approx}^{\prime(\text{SPH})} \\ +f_{1(1)} \hat{\mathbf{t}}_{\approx}^{\prime(1)} & -f_{1(1)} \hat{\mathbf{t}}_{\approx}^{\prime(1)} \end{bmatrix} & \begin{bmatrix} f_{1(2)}f_{2\approx} \mathbf{t}_{\approx}^{\prime(\text{SPH})} & f_{1(2)}f_{2\approx} \mathbf{t}_{\approx}^{\prime(\text{SPH})} \\ +0 & +0 \end{bmatrix} \\ \begin{bmatrix} f_{1(1)}f_{1\approx} \mathbf{t}_{\approx}^{\prime(\text{SPH})} & f_{2(1)}f_{1\approx} \mathbf{t}_{\approx}^{\prime(\text{SPH})} \\ +0 & +0 \end{bmatrix} & \begin{bmatrix} -f_{1(2)}f_{1\approx} \mathbf{t}_{\approx}^{\prime(\text{SPH})} & -f_{2(2)}f_{1\approx} \mathbf{t}_{\approx}^{\prime(\text{SPH})} \\ -f_{2(2)} \hat{\mathbf{t}}_{\approx}^{\prime(2)} & +f_{2(2)} \hat{\mathbf{t}}_{\approx}^{\prime(2)} \end{bmatrix} \\ \begin{bmatrix} f_{1(1)}f_{1\approx} \mathbf{t}_{\approx}^{\prime(\text{SPH})} & f_{2(1)}f_{1\approx} \mathbf{t}_{\approx}^{\prime(\text{SPH})} \\ +0 & +0 \end{bmatrix} & \begin{bmatrix} -f_{1(2)}f_{1\approx} \mathbf{t}_{\approx}^{\prime(\text{SPH})} & -f_{2(2)}f_{1\approx} \mathbf{t}_{\approx}^{\prime(\text{SPH})} \\ +f_{1(2)} \hat{\mathbf{t}}_{\approx}^{\prime(2)} & -f_{1(2)} \hat{\mathbf{t}}_{\approx}^{\prime(2)} \end{bmatrix} \end{bmatrix}, \quad (31)$$

with $\sum_{\pi'J} \mathbf{F}_{\approx}^{\pi I \pi' J} = 0$ and $\sum_I \sum_{\pi I} f_I f_{\pi(I)} \mathbf{F}_{\approx}^{\pi I \pi' J} = 0$, since $f_{1(I)} + f_{2(I)} = 1$ for $I = 1, 2$. In comparison, the related 2×2 matrix of the (TFA) influence operators reads as

$$\mathbf{F}_{\approx \text{TFA}}^{\pi I \pi' J} = \begin{bmatrix} -f_2 \mathbf{t}'^{\text{SPH}}_{\approx} & f_2 \mathbf{t}'^{\text{SPH}}_{\approx} \\ f_1 \mathbf{t}'^{\text{SPH}}_{\approx} & -f_1 \mathbf{t}'^{\text{SPH}}_{\approx} \end{bmatrix}.$$

The intra-crystalline contributions in the (HML) scheme only concern the 2×2 diagonal blocs in Eq. (31). A 4×4 matrix similar to Eq. (31) also holds for a mosaic crystal, with

- (i) the summation over (I) vanishing instead of that over α ;
- (ii) \mathbf{t}'^{SPH} replaced by $\mathbf{t}'^{(G)}_{\approx} = \sum_{\alpha} f_{\alpha} \sum_{\pi(\alpha)} f_{\pi(\alpha)} \mathbf{t}'^{\pi(\alpha)}_{\approx} = \sum_{\alpha} f_{\alpha} \hat{\mathbf{t}}'^{(\alpha)}_{\approx}$ (no grain-like domain shape); and
- (iii) the volume fractions f_{α} a function of the relative slip amplitudes.⁸

The case of a mosaic bi-crystal results in a 8×8 matrix of operators that is obtained from two diagonal blocs of 4×4 dimension like that given in Eq. (31), and complemented by two 4×4 off-diagonal blocs for the inter-granular interactions.

In both cases represented by the 4×4 matrix of Eq. (31), the summation over the 2^4 operators that yields $H0^{\text{TFA-HML}}$ from Eq. (30) rearranges so that, with $\bar{P}0^{IJ} = f_{IJ} P0^{IJ}$ and with $\mathbf{t}'^{(\cdot)}$ standing for either \mathbf{t}'^{SPH} or $\mathbf{t}'^{(G)}$,

$$\begin{aligned} H0^{\text{TFA-HML}} &= f_1 f_2 ((\bar{P}0^{11} R^{11} + \bar{P}0^{21} R^{21}) - (\bar{P}0^{12} R^{12} + \bar{P}0^{22} R^{22})) \\ &\quad \otimes ((\bar{P}0^{11} R^{11} + \bar{P}0^{21} R^{21}) - (\bar{P}0^{12} R^{12} + \bar{P}0^{22} R^{22})) :: \hat{\mathbf{t}}'^{(\cdot)}_{\approx} \\ &\quad - f_1 f_{11} f_{21} ((P0^{11} R^{11} - P0^{21} R^{21}) \otimes (P0^{11} R^{11} - P0^{21} R^{21})) :: \hat{\mathbf{t}}'^{(1)}_{\approx} \\ &\quad - f_2 f_{12} f_{22} ((P0^{22} R^{22} - P0^{12} R^{12}) \otimes (P0^{22} R^{22} - P0^{12} R^{12})) :: \hat{\mathbf{t}}'^{(2)}_{\approx}. \end{aligned} \tag{32a}$$

If the terms $P0^{IJ}$ do not carry any heterogeneity, whether it may come from disorientations or from CRSS heterogeneities within grains and between grains, then $H0^{\text{TFA-HML}} = 0$, $\forall \mathbf{t}'^{(\cdot)}$, $\hat{\mathbf{t}}'^{(1)}$, $\hat{\mathbf{t}}'^{(2)}$ as expected for a homogeneous crystal. The modulus $H0^{\text{TFA-HML}}$ is also zero for two crystals in situations that are symmetric with regard to the applied loading.

Now, in general, one slip plane dominates in each sub-domain, then in each grain, and finally in the bi-crystal. Let us for example take in Eq. (32a) the term (1I) (resp. (1 α)) as dominant in each grain (I) of a bi-crystal (resp. in each sub-domain α of a mosaic crystal), and the term (11) in grain or sub-domain (1) as dominating the term (12) in grain or sub-domain (2) so that $f_{12} \ll f_{11}$ while $P0^{12} \ll P0^{11}$. One thus obtains

$$H0^{\text{TFA-HML}} \approx f_1 f_2 (\bar{P}0^{11} R^{11} \otimes \bar{P}0^{11} R^{11}) :: (f_2 f_{12} \hat{\mathbf{t}}'^{(12)}_{\approx}) \approx 0, \tag{32b}$$

⁸We have here used $f_{\alpha} = \frac{P0^{1(\alpha)} + P0^{2(\alpha)}}{P0^{1(1)} + P0^{2(1)} + P0^{1(2)} + P0^{2(2)}}$, resp. $f_{\alpha(I)}$, $\forall I$.

Table 3

The grain and sub-grain slip system orientations used in the numerical simulations

Crystal	$\theta(x_1, n_1)$	$\phi(x_1, m_1)$	$\theta(x_1, n_2)$	$\phi(x_1, m_2)$
A1	0.81π	$0.81\pi + 0.5\pi$	0.4766666666π	$0.4766666666\pi - 0.5\pi$
A	0.8π	$0.8\pi + 0.5\pi$	0.4666666666π	$0.4666666666\pi - 0.5\pi$
A2	0.79π	$0.79\pi + 0.5\pi$	0.4566666666π	$0.4566666666\pi - 0.5\pi$
B1	0.76π	$0.76\pi + 0.5\pi$	0.4266666666π	$0.4266666666\pi - 0.5\pi$
B	0.75π	$0.75\pi + 0.5\pi$	0.4166666666π	$0.4166666666\pi - 0.5\pi$
B2	0.74π	$0.74\pi + 0.5\pi$	0.4066666666π	$0.4066666666\pi - 0.5\pi$
S	$2\pi/3$	$2\pi/3 + 0.5\pi$	$\pi/3$	$\pi/3 - 0.5\pi$

because $f_1 f_{11} f_{21} (P0^{11} R^{11} \otimes P0^{11} R^{11}) :: (f_{11} \mathbf{t}^{\prime 11}) = f_2 f_{12} f_{22} (P0^{12} R^{12} \otimes P0^{12} R^{12}) :: (f_{12} \mathbf{t}^{\prime 12}) = 0$. It is then analytically verified from a simple example that the stiffness contributions which do not totally cancel or compensate each other are those of minor importance.

Fig. 6(a) and (b) report tensile stress–strain curves (Σ, E) obtained for the mosaic bi-crystal structures considered here, under the mixed loading conditions $dE_{11} = d\varepsilon$, $d\Sigma_{ij} = 0$, $\forall ij \neq 11$. The prescribed strain axis is x_1 and, as in Fig. 1, all slip planes contain the x_3 -axis while all their slip directions are in the x_1 – x_2 plane. The considered slip system orientations are specified in Table 3 through the angles of the slip direction and of the slip plane normal to the x_1 -axis ($\theta^{g(\alpha(I))} = (x_1, \mathbf{n}^{g(\alpha(I))})$, $\phi^{g(\alpha(I))} = (x_1, \mathbf{m}^{g(\alpha(I))})$). For all domains, a zero total rotation is assumed, i.e. $d\tilde{\omega}_{\alpha(I)}^{\text{el}} = -d\tilde{\omega}_{\alpha(I)}^{\text{pl}}$. Since the rotation vector is along the x_3 frame direction, one obtains $d\tilde{\omega}_{\alpha(I)}^{\text{pl}} = (0, 0, (d\gamma^{2(\alpha(I))} - d\gamma^{1(\alpha(I))})/2)$. The slip system orientations are step-wise updated using $d\mathbf{n}^{g(\alpha(I))} = d\tilde{\omega}_{\alpha(I)}^{\text{el}} \wedge \mathbf{n}^{g(\alpha(I))}$ (resp. $d\mathbf{m}^{g(\alpha(I))}$). All performed simulations, which do not aim at matching experimental data, make use of a local, non-linear and non-convex physical hardening law of the form (for $g = 1, 2$).

$$d\tau_c^g = \sum_k h^{gk} d\gamma^k = \sum_k 2h_0(1 - R) \left[\frac{(a - (a - 1)\delta^{gk}) + c\gamma^{\text{Max}} + q(\Gamma - \gamma^{\text{Max}})}{\tau_c^g + \tau_c^k} \right] d\gamma^k, \quad (33)$$

with in each domain, $\Gamma = \sum_k \gamma^k$, $\gamma^{\text{Max}} = \max(\gamma^k)$,

$$R = \begin{cases} 0, & \text{for } \langle \tau_c \rangle < \tau_{0II}, \\ \left(\frac{\langle \tau_c \rangle - \tau_{0II}}{\tau_s - \tau_{0II}} \right), & \text{if } \langle \tau_c \rangle \in (\tau_{0II}, \tau_s). \end{cases}$$

In the hardening law of Eq. (33), the coefficient $a > 1$ introduces an initial hardening anisotropy which decreases slowly during single slip ($\Gamma = \gamma^{\text{Max}}$) and faster when multiple slip operates ($\Gamma > \gamma^{\text{Max}}$), according respectively to the $c \approx a$ and to the $q \gg a$ coefficient. The single crystal reference curves in Fig. 6(a) and (b) typically exhibit a first single slip stage (I) followed by a stiffer double slip stage (II), as in FCC crystals but not only in those. This results in a concave behavior. The “recovery function” R then progressively reduces the

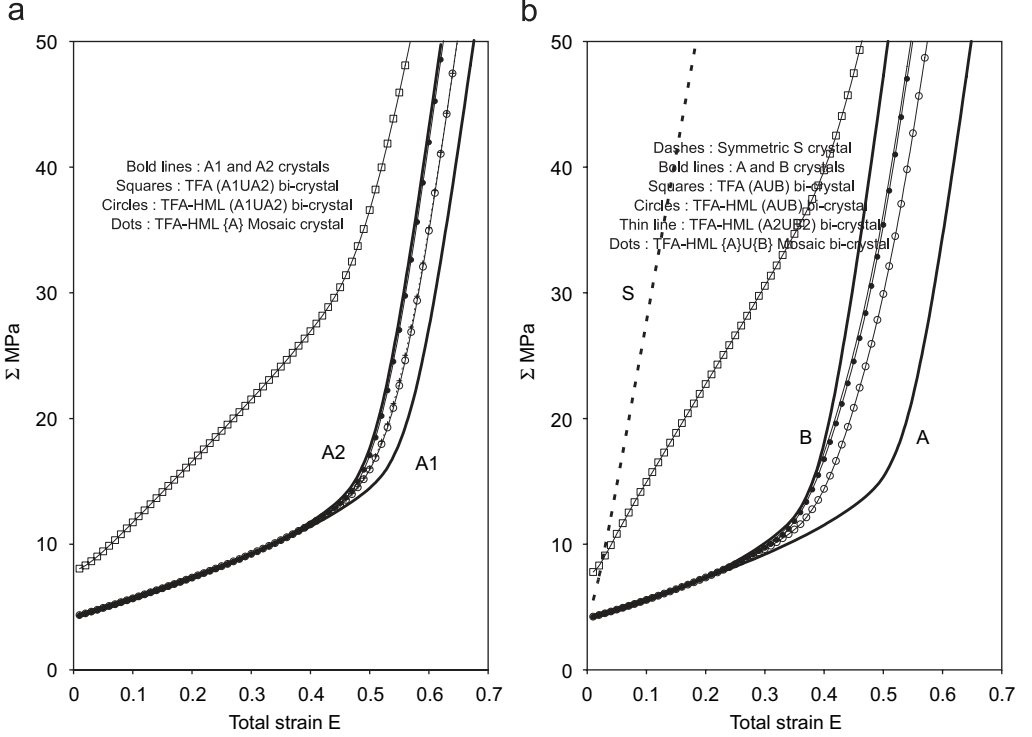


Fig. 6. Simulated stress–strain curves for bi-crystals using the (RSL-TFA) and (RSL-TFA-HML) modeling for (a) $A1$ and $A2$ closely oriented grains and (b) A and B grains.

Table 4

The elasticity and hardening parameter values which are used for the numerical simulations (Eq. (33))

Elasticity and yield	$\mu = 30$ GPa	$\nu = 0.3$	$\tau_{c0} = 2$ MPa	$\tau_{c0}II = 35$ MPa	$\tau_s = 45$ MPa
Hardening	$h_0 = 48$	$A = 4$	$c = 2$	$q = 900$	$n = 20$

μ and ν are respectively the elastic shear modulus and the Poisson's ratio.

stage-II hardening according to a Voce-type law, with $\langle \tau_c \rangle = \sum_i f_i \sum_{\alpha I} f_{\alpha I} \sum_{g(\alpha I)} f_{g(\alpha I)} \tau_c^{g(\alpha I)}$ as reference CRSS value; note that stage III, and subsequent stages (Franciosi, 1994), are ignored. The values given to the elasticity and hardening moduli in the reported simulations are collected in Table 4.

Fig. 6(a) reports a comparison of the stress–strain curves that result from the (RSL-TFA) and the (RSL-TFA-HML) modeling for a bi-crystal ($A1 \cup A2$) with ($f_{A1} = f_{A2} = 0.5$). This bi-crystal is made of two closely oriented grain types ($A1$) and ($A2$), with crystal ($A2$) stiffer than crystal ($A1$) since it is closer to a symmetric orientation (S). The mean orientation of crystal ($A2$) corresponds to that of a (A) crystal. The bi-crystal ($A1 \cup A2$) is therefore a heterogeneous description of crystal (A). The figure also reports a stress–strain curve obtained from the (RSL-TFA-HML) modeling for the mosaic

crystal $\{A\} = \{A1 \cup A2\}$, which is not a heterogeneous representation of crystal (A) since the sub-domains have unequal and evolving volume fractions

$$\left(1 > \frac{f_{A1}(\varepsilon)}{f_{A2}(\varepsilon)} = \frac{P0^{1A1}(\varepsilon) + P0^{2A1}(\varepsilon)}{P0^{1A2}(\varepsilon) + P0^{2A2}(\varepsilon)} \rightarrow 0 \right).$$

Fig. 6(b) corresponds to similar plots for a bi-crystal ($A \cup B$) with ($f_A = f_B = 0.5$), made of two highly disoriented grains (A) and (B), with crystal (B) stiffer than crystal (A) since it is closer to the symmetric orientation (S). The orientations of the (A) and (B) crystals are too different to be regarded as components of a mosaic crystal $\{A \cup B\}$, but, considering two mosaic crystals $\{A\} = \{A1 \cup A2\}$, and $\{B\} = \{B1 \cup B2\}$, a plot of the (RSL-TFA-HML) behavior estimate for the mosaic bi-crystal ($\{A\} \cup \{B\}$) is also reported.

On both figures, it is first seen that, compared to the individual behaviors of the constitutive phases (i.e. crystal pairs ($(A1)$, ($A2$)) and ((A) , (B)), respectively), the (RSL-TFA) estimate for the stiffness of the corresponding bi-crystal is stiffer than the stiffest constitutive phase, while that obtained from the (RSL-TFA-HML) scheme well is of intermediate value. The (RSL-TFA-HML) estimate for the stiffness of the mosaic crystal $\{A\} = \{A1 \cup A2\}$ in Fig. 6(a) is also between the estimates for the stiffness of the constitutive two phases, but this is a case for which the (RSL-TFA) modeling does not provide a direct comparison. The (RSL-TFA-HML) estimate for the stiffness of the mosaic crystal $\{A\}$ is greater than that of the bi-crystal ($A1 \cup A2$) but it also remains between the stiffness of the crystals ($A1$) and ($A2$), although it approaches the stiffness of crystal ($A2$) with the increase of the volume fraction f_{A2} .

In Fig. 6(b), the plot of the (RSL-TFA-HML) estimate for the stiffness of the mosaic bi-crystal ($\{A\} \cup \{B\}$) appears stiffer than that for the bi-crystal ($A \cup B$) and approaches that for the bi-crystal ($A2 \cup B2$) since the estimate for the stiffness of the mosaic crystal $\{A\}$ (resp. $\{B\}$) approaches that of the crystal ($A2$) (resp. ($B2$)). Fig. 7(a) and (7b), respectively present a zoom of Fig. 6(a) and 6(b), with further comments including some ‘‘bound’’ considerations. In Fig. 7(a), the comparison of the stiffness of crystal (A) with the (RSL-TFA-HML) estimate for the stiffness of the bi-crystal ($A1 \cup A2$), of same mean orientation, is a measure of the difference ($H0_\Sigma - H0^{(h,\phi)}$) between a homogeneous and a heterogeneous crystal data analysis. That difference is close to zero as expected for a validation of the proposed (HML) modeling for application to intra-crystalline plasticity.

Stress–strain curves that have been estimated under the assumption of uniform total axial strain (denoted by (L)), are reported in Fig. 7(a) in the case of the bi-crystal ($A1 \cup A2$), and in Fig. 7(b) in the case of both bi-crystals ($A \cup B$) and ($A2 \cup B2$). The (L) estimate for the bi-crystal ($A2 \cup B2$) is an overvalued approximation of the (L) estimate for the mosaic bi-crystal ($\{A\} \cup \{B\}$), the latter being unknown. This (L) estimate is a close approximation of the Lin-Taylor estimate,⁹ which is a 1st order upper bound for elastic-plastic behavior laws that derive from a convex plastic potential (Ponte-Castaneda and Suquet, 1998). Here, although the behavior law is concave (see Eq. (33)), all the (RSL-TFA-HML) estimates for the bi-crystals ($A1 \cup A2$), ($A \cup B$) and ($A2 \cup B2$) seem to be below their related (L) estimate.

These comparisons are sufficient to establish that the proposed (RSL-TFA-HML) scheme for poly-crystal plasticity is noticeably more correct than that obtained by the

⁹The plastic strain is zero in the x_3 direction such that $dE_{22} \approx dE_{22}^p = -dE_{11}^p \approx -dE_{11}$, but $dE_{22}^L = -\nu dE_{11}^L$.

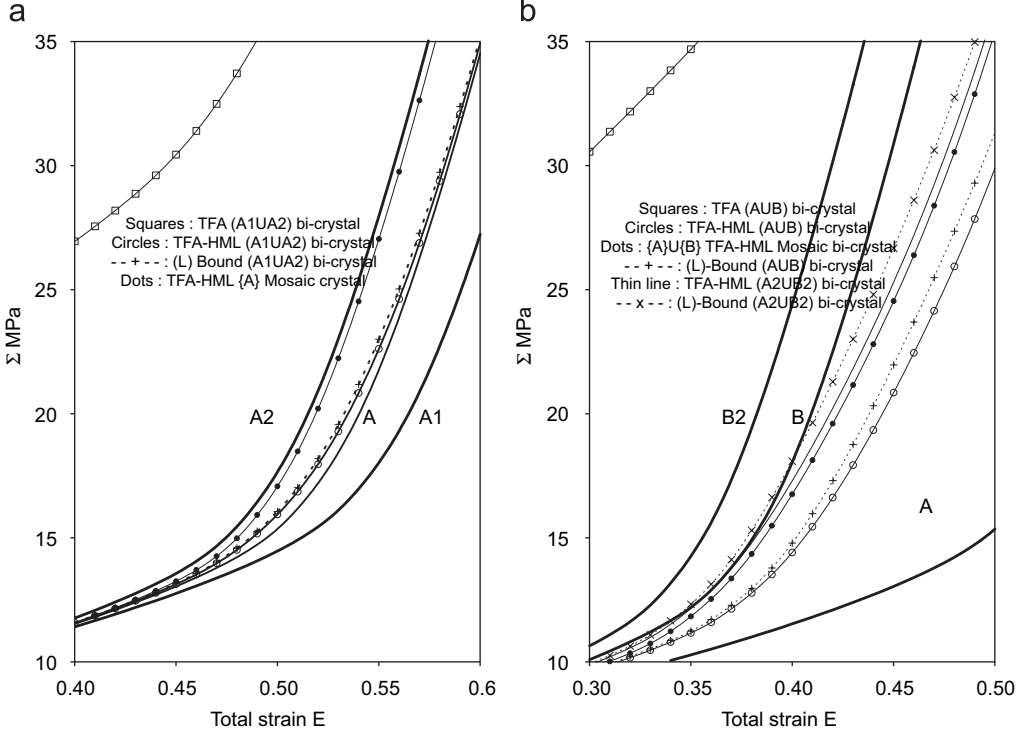


Fig. 7. Zoom of Fig. 6 comparing different (TFA-HML) estimates of single and bi-crystals, and (TFA-HML) estimates with (L)-estimates for (a) (A1UA2), and (b) (AUB) and (A2UB2) bi-crystals.

(RSL-TFA) as far as stiffness estimates are concerned. Slip-induced disorientations in perfect crystals can also be initiated, as we have verified, by introducing a slight heterogeneity between the initial CRSSs $\tau_{c0}^{\pi(I)}$ of the sub-domains. But further evolutions intimately involve the type of hardening law and will not be commented upon here. Clearly, the orthogonality property between the laminate operators and the slip system Schmid tensors in the HML slip structures makes the over-stiffness due to TFA mostly vanish, if an appropriate superposition of the elementary solutions is performed. Taking the RSL as flow condition, this result agrees with the coupled non-uniform TFA (NTFA) of Michel and Suquet (2004) which also called for “orthogonal” plastic modes to lower the stiffness excess from the TFA.

The consideration of HESCs to represent poly-crystals legitimates the use of both the RSL as flow criterion and the HML structure as slip organization for aggregate plasticity. But it is noteworthy that the proposed (HML) scheme for slip also appears relevant for describing polycrystal plasticity within the TFA framework independently of the chosen flow criterion.

5. Conclusion

Stress and strain heterogeneities in heterogeneous crystals and in polycrystals have been taken into account in using the transformation field analysis (TFA) as homogenization

framework, coupled with an extension of the crystal regularized Schmid law (RSL) as plastic flow criterion. The intra-crystalline slip activity is described as organized into multi-laminate structures. It has been demonstrated that laminate layers either parallel to slip planes or perpendicular to slip directions do not contribute to the over-stiffness caused by the TFA. Hence, we have considered hierarchical multi-laminate (HML) structures where each successive lamination is parallel to a different slip plane orientation. Through a careful accounting of all possible slip planes hierarchies as heterogeneous plastic strain modes, we have shown that, for an appropriately weighted superposition of all modes with regard to relative slip plane activities, most of the over-stiffness due to the TFA vanishes. A relevant extension to poly-crystals of this (RSL-TFA-HML) modeling has been proposed and numerically illustrated.

Acknowledgments

The authors are very grateful to Gilles Francfort for his fruitful comments on this manuscript, and they also thank Anne-Gaëlle Adam and Pierre Barroy for their help with the corrections.

Appendix A. The stress operators in the TFA applied to aggregates

Let v^I be an elastic (ellipsoidal) heterogeneity with moduli $\underline{\underline{\mathbf{C}}}^I$ supporting uniform eigenstrains $\underline{\underline{\boldsymbol{\varepsilon}}}^{oI}$ in an infinite elastic matrix with moduli $\underline{\underline{\mathbf{C}}}^M$ possibly supporting uniform eigenstrains $\underline{\underline{\boldsymbol{\varepsilon}}}^{oM}$ as well. In the TFA, $\underline{\underline{\boldsymbol{\varepsilon}}}^{oI}$ is a plastic strain tensor $\underline{\underline{\boldsymbol{\varepsilon}}}^{PI}$. The (uniform) strain solution $\underline{\underline{\boldsymbol{\varepsilon}}}^I$ in \mathbf{v}^I (Eshelby, 1957) satisfies

$$\underline{\underline{\boldsymbol{\sigma}}}^I = \underline{\underline{\mathbf{C}}}^I : \left(\underline{\underline{\boldsymbol{\varepsilon}}}^I - \underline{\underline{\boldsymbol{\varepsilon}}}^{oI} \right) = \underline{\underline{\mathbf{C}}}^I : \left(\Delta \underline{\underline{\boldsymbol{\varepsilon}}}^I - \Delta \underline{\underline{\boldsymbol{\varepsilon}}}^{oI} \right) = \underline{\underline{\mathbf{C}}}^{MI} : \Delta \underline{\underline{\boldsymbol{\varepsilon}}}^I - \underline{\underline{\mathbf{p}}}^{*I}. \quad (\text{A.1})$$

Applying the uniform strain tensor $\underline{\underline{\mathbf{E}}}$ from infinity yields $\Delta \underline{\underline{\boldsymbol{\varepsilon}}}^I = \Delta \underline{\underline{\mathbf{E}}} + \underline{\underline{\mathbf{t}}}^I : \underline{\underline{\mathbf{p}}}^{*I}$ in terms of polarization stresses $\underline{\underline{\mathbf{p}}}^{*I}$, where $\Delta \underline{\underline{\boldsymbol{\varepsilon}}} = (\underline{\underline{\boldsymbol{\varepsilon}}} - \underline{\underline{\boldsymbol{\varepsilon}}}^{oM})$ and $\underline{\underline{\mathbf{t}}}^I$ is the (uniform) modified Green operator integral over I . For volume fractions f_I of several inclusion types indexed by (I) , with $\sum_I f_I = 1 - f_M$, one obtains a system of linear equations that involves the spatial distribution of inclusions. Assume ellipsoidal symmetry for the distribution of inclusion pairs. Then

$$\Delta \underline{\underline{\boldsymbol{\varepsilon}}}^I = \Delta \underline{\underline{\mathbf{E}}} - \underline{\underline{\mathbf{t}}}^D : \left\langle \underline{\underline{\mathbf{p}}}^* \right\rangle + \underline{\underline{\mathbf{t}}}^I : \underline{\underline{\mathbf{p}}}^{*I}, \quad (\text{A.2})$$

where $\underline{\underline{\mathbf{t}}}^D$ is the characteristic Green operator integral (Ponte-Castaneda and Willis, 1995) and “ $\langle \cdot \rangle$ ” denotes $\sum_I f_I \langle \cdot \rangle^I$. Eliminating $\Delta \underline{\underline{\boldsymbol{\varepsilon}}}^I$ from Eqs. (A.1) and (A.2) yields, with $\Delta \underline{\underline{\mathbf{C}}}^{M/I} = \underline{\underline{\mathbf{C}}}^M - \underline{\underline{\mathbf{C}}}^I$:

$$\underline{\underline{\mathbf{p}}}^{*I} = \left(\underline{\underline{\mathbf{I}}} - \Delta \underline{\underline{\mathbf{C}}}^{M/I} : \underline{\underline{\mathbf{t}}}^I \right)^{-1} : \left(\Delta \underline{\underline{\mathbf{C}}}^{M/I} : \left(\Delta \underline{\underline{\mathbf{E}}} - \underline{\underline{\mathbf{t}}}^D : \left\langle \underline{\underline{\mathbf{p}}}^* \right\rangle \right) + \underline{\underline{\mathbf{C}}}^I : \Delta \underline{\underline{\boldsymbol{\varepsilon}}}^{oI} \right). \quad (\text{A.3})$$

Solving first Eq. (A.3) for $\langle \tilde{\mathbf{p}}^* \rangle$, then for each stress tensor $\tilde{\mathbf{p}}^{*I}$, we get

$$\tilde{\mathbf{p}}^{*I} = \tilde{\mathbf{q}}^I : \Delta \tilde{\mathbf{E}} + \sum_J \tilde{\mathbf{r}}^{IJ} : \Delta \tilde{\boldsymbol{\varepsilon}}^{oJ}, \quad \langle \tilde{\mathbf{p}}^* \rangle = \langle \tilde{\mathbf{q}} \rangle : \Delta \tilde{\mathbf{E}} + \sum_J \langle \tilde{\mathbf{r}} \rangle^J : \Delta \tilde{\boldsymbol{\varepsilon}}^{oJ}, \quad (\text{A.4})$$

$$\Delta \tilde{\boldsymbol{\varepsilon}}^I = \left(\Delta \tilde{\mathbf{C}}^{M/I} \right)^{-1} : \left(\tilde{\mathbf{p}}^{*I} - \tilde{\mathbf{C}}^I : \Delta \tilde{\boldsymbol{\varepsilon}}^{oJ} \right) = \tilde{\mathbf{A}}^I : \Delta \tilde{\mathbf{E}} + \sum_J f_J \tilde{\mathbf{D}}^{IJ} : \Delta \tilde{\boldsymbol{\varepsilon}}^{oJ}. \quad (\text{A.5a})$$

$$\begin{aligned} \tilde{\boldsymbol{\sigma}}^I &= \tilde{\mathbf{C}}^I : \left(\left(\tilde{\mathbf{A}}^I : \left(\tilde{\mathbf{S}}^{\text{eff}} : \tilde{\boldsymbol{\Sigma}} + \Delta \tilde{\mathbf{E}}^o \right) + \sum_J f_J \tilde{\mathbf{D}}^{IJ} : \Delta \tilde{\boldsymbol{\varepsilon}}^{oJ} \right) - \Delta \tilde{\boldsymbol{\varepsilon}}^{oI} \right) \\ &= \tilde{\mathbf{B}}^I : \tilde{\boldsymbol{\Sigma}} + \sum_J f_J \tilde{\mathbf{F}}^{IJ} : \Delta \tilde{\boldsymbol{\varepsilon}}^{oJ}. \end{aligned} \quad (\text{A.5b})$$

Taking as effective eigenstrains $\Delta \tilde{\mathbf{E}}^o = \sum_J f_J \tilde{\mathbf{B}}^{IJ} : \Delta \tilde{\boldsymbol{\varepsilon}}^{oJ}$ (see Levin, 1967), one can write

$$f_J \tilde{\mathbf{F}}^{IJ} = \tilde{\mathbf{C}}^I : \left(f_J \tilde{\mathbf{D}}^{IJ} - \mathbf{I} \delta^{IJ} \right) + \tilde{\mathbf{C}}^I : \tilde{\mathbf{A}}^I : f_J \tilde{\mathbf{B}}^{IJ} = \tilde{\mathbf{H}}^I \delta^{IJ} - f_J \tilde{\mathbf{L}}^{IJ}. \quad (\text{A.6})$$

Next, with $\tilde{\mathbf{T}}^I = \left(\left(\Delta \tilde{\mathbf{C}}^{M/I} \right)^{-1} - \tilde{\mathbf{t}}^I \right)^{-1}$, $\tilde{\mathbf{K}}^I = \tilde{\mathbf{T}}^I : \left(\Delta \tilde{\mathbf{C}}^{M/I} \right)^{-1} = \tilde{\mathbf{I}} + \tilde{\mathbf{T}}^I : \tilde{\mathbf{t}}^I$, $\tilde{\mathbf{t}}^I : \tilde{\mathbf{K}}^I = \tilde{\mathbf{K}}^{II} : \tilde{\mathbf{t}}^I$ in Eq. (A.3):

$$\begin{aligned} \tilde{\mathbf{p}}^{*I} &= \tilde{\mathbf{T}}^I : \left(\tilde{\mathbf{I}} + \tilde{\mathbf{t}}^D : \langle \tilde{\mathbf{T}} \rangle \right)^{-1} : \left(\Delta \tilde{\mathbf{E}} - \tilde{\mathbf{t}}^D : \langle \tilde{\mathbf{K}} : \tilde{\mathbf{C}} : \Delta \tilde{\boldsymbol{\varepsilon}}^o \rangle \right) + \tilde{\mathbf{K}}^I : \tilde{\mathbf{C}}^I : \Delta \tilde{\boldsymbol{\varepsilon}}^{oI}, \\ f_J \tilde{\mathbf{D}}^{IJ} &= \tilde{\mathbf{t}}^I : \tilde{\mathbf{r}}^{IJ} - \tilde{\mathbf{t}}^D : \langle \tilde{\mathbf{r}} \rangle^J, \\ &= \tilde{\mathbf{t}}^I : \left(\mathbf{I} \delta^{IJ} - \tilde{\mathbf{q}}^I : \tilde{\mathbf{t}}^D f_J \right) : \tilde{\mathbf{K}}^J : \tilde{\mathbf{C}}^J - \tilde{\mathbf{t}}^D : \left(\mathbf{I} - \langle \tilde{\mathbf{q}} \rangle : \tilde{\mathbf{t}}^D \right) : f_J \tilde{\mathbf{K}}^J : \tilde{\mathbf{C}}^J. \end{aligned} \quad (\text{A.7})$$

Then, from Eq. (A.7) in Eq. (A.6), with $\tilde{\mathbf{A}}^I = \tilde{\mathbf{K}}^{II} : \left(\tilde{\mathbf{I}} + \tilde{\mathbf{t}}^D : \langle \tilde{\mathbf{T}} \rangle \right)^{-1}$ and $\tilde{\mathbf{B}}^I = \tilde{\mathbf{C}}^I : \tilde{\mathbf{A}}^I : \tilde{\mathbf{S}}^{\text{eff}}$, we obtain

$$\begin{aligned} f_J \tilde{\mathbf{F}}^{IJ} &= \tilde{\mathbf{C}}^I : \left(f_J \tilde{\mathbf{D}}^{IJ} - \mathbf{I} \delta^{IJ} \right) + \tilde{\mathbf{C}}^I : \tilde{\mathbf{A}}^I : f_J \tilde{\mathbf{B}}^{IJ} \\ &= \tilde{\mathbf{C}}^I : \left(\tilde{\mathbf{t}}^I : \tilde{\mathbf{K}}^I : \tilde{\mathbf{C}}^I - \mathbf{I} \right) \delta^{IJ} - \tilde{\mathbf{C}}^I : \tilde{\mathbf{A}}^I : \left(\tilde{\mathbf{B}}^{IJ} - \tilde{\mathbf{t}}^D : \tilde{\mathbf{K}}^J : \tilde{\mathbf{C}}^J \right), \end{aligned}$$

which gives, after some algebra and noticing that $\tilde{\mathbf{K}}^J : \tilde{\mathbf{C}}^J$ equals $\left(\tilde{\mathbf{I}} + \langle \tilde{\mathbf{T}} \rangle : \tilde{\mathbf{t}}^D \right) : \tilde{\mathbf{C}}^{\text{eff}} : \tilde{\mathbf{B}}^{IJ}$:

$$\begin{aligned} \tilde{\mathbf{H}}^I &= \left(\left(\tilde{\mathbf{C}}^M - \left(\tilde{\mathbf{t}}^I \right)^{-1} \right)^{-1} - \left(\tilde{\mathbf{C}}^I \right)^{-1} \right)^{-1} \\ &= -\tilde{\mathbf{C}}^I : \left(\mathbf{I} - \tilde{\mathbf{t}}^I : \Delta \tilde{\mathbf{C}}^{M/I} \right)^{-1} : \left(\mathbf{I} - \tilde{\mathbf{t}}^I : \tilde{\mathbf{C}}^M \right) = \tilde{\mathbf{H}}^I, \end{aligned} \quad (\text{A.8a})$$

$$\tilde{\mathbf{L}}^{IJ} = -\tilde{\mathbf{B}}^I : \tilde{\mathbf{X}} : \tilde{\mathbf{B}}^{IJ}, \quad \tilde{\mathbf{X}} = \tilde{\mathbf{C}}^{\text{eff}} - \tilde{\mathbf{C}}^{\text{eff}} : \tilde{\mathbf{N}} : \tilde{\mathbf{C}}^{\text{eff}}, \quad \tilde{\mathbf{N}} = \tilde{\mathbf{t}}^D + \tilde{\mathbf{t}}^D : \langle \tilde{\mathbf{T}} \rangle : \tilde{\mathbf{t}}^D. \quad (\text{A.8b})$$

This solution includes the self-consistent scheme for aggregates, when $f_M \rightarrow 0$, all inclusions are congruent ($\mathbf{t}^I = \mathbf{t}^i, \forall I$) and in a shape-homothetic distribution $\mathbf{t}^D = \mathbf{t}^i$, and with \mathbf{C}^{eff} replacing \mathbf{C}^M . Since $\langle \mathbf{T} \rangle = \mathbf{0}$, then $\mathbf{N} = \mathbf{t}^i$ and $\mathbf{X} = \mathbf{C}^{\text{eff}} - \mathbf{C}^{\text{eff}} : \mathbf{t}^i : \mathbf{C}^{\text{eff}} = \mathbf{t}^i$ (the dual stress Green operator to \mathbf{t}^i), while from Eq. (A.8a) $\mathbf{H}^I = -\mathbf{C}^I : \mathbf{A}^I : (\mathbf{I} - \mathbf{t}^i : \mathbf{C}^{\text{eff}}) = -\mathbf{B}^I : \mathbf{C}^{\text{eff}} : (\mathbf{I} - \mathbf{t}^i : \mathbf{C}^{\text{eff}}) = -\mathbf{B}^I : \mathbf{t}^i = \mathbf{H}^I = -\mathbf{t}^i : \mathbf{B}^I$. This yields $\mathbf{L}^{IJ} = -\mathbf{B}^I : \mathbf{t}^i : \mathbf{B}^J = \mathbf{H}^I : \mathbf{B}^J = \mathbf{B}^I : \mathbf{H}^J$, and finally $f_J \mathbf{F}^{IJ} = \mathbf{H}^I : (\mathbf{I} \delta^{IJ} - f_J \mathbf{B}^J) = (\mathbf{I} \delta^{IJ} - f_J \mathbf{B}^I) : \mathbf{H}^J$. Further manipulations of \mathbf{H}^I yield Dvorak's result (1992):

$$f_J \mathbf{F}^{IJ} = (\mathbf{B}^I - \mathbf{I}) : (\mathbf{S}^I - \mathbf{S}^{\text{eff}})^{-1} : (\mathbf{I} \delta^{IJ} - f_J \mathbf{B}^J); \quad \mathbf{S}^I = (\mathbf{C}^I)^{-1}, \quad \mathbf{S}^{\text{eff}} = (\mathbf{C}^{\text{eff}})^{-1}. \quad (\text{A.9})$$

With $(\Delta \mathbf{S}^{\text{eff}/I})^{-1} = (\mathbf{S}^{\text{eff}} - \mathbf{S}^I)^{-1}$ related to $(\Delta \mathbf{C}^{\text{eff}/I})^{-1}$ in the same manner as \mathbf{t}^i is related to \mathbf{t}^i , \mathbf{H}^I is given by

$$\mathbf{H}^I = -\mathbf{C}^I : \left(\mathbf{I} - \mathbf{S}^{\text{eff}} : (\Delta \mathbf{S}^{\text{eff}/I})^{-1} \right) : \left(\mathbf{t}^i - (\Delta \mathbf{S}^{\text{eff}/I})^{-1} \right)^{-1} : \mathbf{t}^i = -\mathbf{t}^i : \mathbf{Y}^I : \mathbf{t}^i, \quad (\text{A.10})$$

where

$$\mathbf{Y}^I = \mathbf{Y}^{Ii} = \left(\mathbf{t}^i - \mathbf{t}^i : \Delta \mathbf{S}^{\text{eff}/I} : \mathbf{t}^i \right)^{-1}.$$

In the presence of a matrix phase, $\langle \mathbf{\sigma} \rangle + f_M \mathbf{\sigma}^M = \mathbf{\Sigma}$ and the operators \mathbf{F}^{IM} are connected through Eq. (A.5b) which becomes $\sum_J f_J \mathbf{F}^{IJ} + f_M \mathbf{F}^{IM} = \mathbf{0}, \forall I$. Homogeneous elasticity \mathbf{C}^M yields $\mathbf{A}^I = \mathbf{B}^I = \mathbf{I}$ and $\mathbf{T}^I = \mathbf{0}$. But $\mathbf{T}^I : (\Delta \mathbf{C}^{M/I})^{-1} = (\mathbf{I} - \Delta \mathbf{C}^{M/I} : \mathbf{t}^I)^{-1} = \mathbf{I}$. Thus,

$$\begin{aligned} \mathbf{H}^I &= \mathbf{C}^M : \mathbf{t}^I : \mathbf{C}^M - \mathbf{C}^M = -\mathbf{t}^I, \\ \mathbf{L}^{IJ} &= -\mathbf{X} = \mathbf{C}^M : \mathbf{t}^D : \mathbf{C}^M - \mathbf{C}^M = -\mathbf{t}^D, \quad \forall (I, J). \end{aligned} \quad (\text{A.11})$$

If furthermore $\mathbf{t}^D = \mathbf{t}^I = \mathbf{t}^i, \forall I$, then $f_I \mathbf{F}^{II} = (1 - f_I) \mathbf{F}_i^M, f_J \mathbf{F}^{JJ} = -f_J \mathbf{F}_i^M$, with $\mathbf{F}_i^M = -\mathbf{t}^i, \forall I, J$. For any two-phase material (I, M) , the 2×2 terms of the matrix $[\mathbf{F}]$ of influence operators are also proportional to the same $\mathbf{F}_i^M \neq -\mathbf{t}^i$ since $\mathbf{\sigma}^I - \mathbf{B}^I : \mathbf{\Sigma} = \mathbf{\sigma}^M - \mathbf{B}^M : \mathbf{\Sigma} = \mathbf{0}$ when $\mathbf{\varepsilon}^{oI} = \mathbf{\varepsilon}^{oM}$. Thus, from Eq. (A.9):

$$\begin{aligned} \mathbf{F}_i^M &= \frac{1}{f_M} (\mathbf{B}^I - \mathbf{I}) : (\mathbf{S}^I - \mathbf{S}^M)^{-1} = (\mathbf{B}^I - \mathbf{B}^M) : (\mathbf{S}^I - \mathbf{S}^M)^{-1} \\ &= \frac{1}{f_I} (\mathbf{B}^M - \mathbf{I}) : (\mathbf{S}^M - \mathbf{S}^I)^{-1}. \end{aligned} \quad (\text{A.12})$$

Similar relations hold for the matrix $\underline{\mathbf{D}}$ in Eqs. (A.5), replacing $\underline{\mathbf{F}}_i^M$ with $\underline{\mathbf{D}}_i^M = \underline{\mathbf{t}}^i : \underline{\mathbf{C}}^M$ and $(\underline{\mathbf{B}}, \underline{\mathbf{S}})$ with $(\underline{\mathbf{A}}, \underline{\mathbf{C}})$. The related column matrix of stress tensors reads as

$$\begin{pmatrix} \underline{\boldsymbol{\sigma}}^I \\ \underline{\boldsymbol{\sigma}}^M \end{pmatrix} = \begin{pmatrix} \underline{\mathbf{B}}^I \\ \underline{\mathbf{B}}^M \end{pmatrix} : \underline{\boldsymbol{\Sigma}} + \begin{pmatrix} (f_M) \underline{\mathbf{F}}_i^M & -(f_M) \underline{\mathbf{F}}_i^M \\ -(1-f_M) \underline{\mathbf{F}}_i^M & (1-f_M) \underline{\mathbf{F}}_i^M \end{pmatrix} : \begin{pmatrix} \underline{\boldsymbol{\varepsilon}}^{oI} \\ \underline{\boldsymbol{\varepsilon}}^{oM} \end{pmatrix}.$$

This expression for the stress tensor $\underline{\boldsymbol{\sigma}}^I$ also holds for the self-consistent modeling of an aggregate, seen as a two-phase $(\underline{\mathbf{C}}^I, \underline{\mathbf{C}}^{\text{eff}})$ inclusion/matrix structure for each grain type separately. The self-consistent approximation $(\underline{\mathbf{I}} - \underline{\mathbf{B}}^I) : (\underline{\mathbf{S}}^I - \underline{\mathbf{S}}^{\text{eff}})^{-1} = \underline{\mathbf{B}}^I : \underline{\mathbf{t}}^i = \underline{\mathbf{B}}^I : \underline{\mathbf{C}}^{\text{eff}} (\underline{\mathbf{I}} - \underline{\mathbf{t}}^i : \underline{\mathbf{C}}^{\text{eff}})$ yields Kröner's elastic accommodation (Kröner, 1961), namely

$$\begin{aligned} \underline{\boldsymbol{\sigma}}^I &= \underline{\mathbf{B}}^I : \underline{\boldsymbol{\Sigma}} - \underline{\mathbf{C}}^I : \underline{\mathbf{A}}^I : (\underline{\mathbf{I}} - \underline{\mathbf{t}}^i : \underline{\mathbf{C}}^{\text{eff}}) : (\underline{\boldsymbol{\varepsilon}}^{PI} - \underline{\mathbf{E}}^P) \\ &= \underline{\mathbf{B}}^I : \underline{\boldsymbol{\Sigma}} - (\underline{\mathbf{I}} - \underline{\mathbf{B}}^I) : (\underline{\mathbf{S}}^I - \underline{\mathbf{S}}^{\text{eff}})^{-1} : (\underline{\boldsymbol{\varepsilon}}^{PI} - \underline{\mathbf{E}}^P). \end{aligned}$$

Appendix B. Elasticity moduli and local stresses in a (3)-HML crystal structure

Consider $P = 4$ slip plane orientations in a crystal of volume V , denoted by A, B, C, D according to their hierarchy $A|B|C|(D)$ in a (3)-HML structure. They are assumed to occupy distinct volume fractions $F_\pi V$ of V , and to possibly have different elasticity moduli $\underline{\mathbf{C}}^\pi$, $\pi = A, B, C, D$, because of lattice disorientations. We denote by $\Delta \underline{\mathbf{C}}^{\pi/\pi'}$ the difference $(\underline{\mathbf{C}}^\pi - \underline{\mathbf{C}}^{\pi'})$, by $\underline{\mathbf{t}}^\pi$ the modified Green operator integral for the π -oriented laminate layers, and by $\underline{\mathbf{F}}_i^M$ the operators $\underline{\mathbf{F}}_i^M$ of Eqs. (A.12) and (A.13) in Appendix A. Note that there is no need to keep the subscript i . With the planes (A) defining the first lamination orientation, and with the second phase of (B) planes taken as matrix, the effective elasticity tensor for this first lamination level reads as $\underline{\mathbf{C}}^{AB} = \underline{\mathbf{C}}^B - f_A ((\Delta \underline{\mathbf{C}}^{B/A})^{-1} - f_B \underline{\mathbf{t}}^A)^{-1}$, where $f_A = F_A / (F_A + F_B) = 1 - f_B$. Next, for a second lamination orientation (B) and upon taking the third phase of (C) planes as the level-2 matrix in which the (AB) homogeneous equivalent medium is embedded, one obtains

$$\underline{\mathbf{C}}^{ABC} = \underline{\mathbf{C}}^C - f_{AB} \left(\left(\Delta \underline{\mathbf{C}}^{C/B} + f_A \left((\Delta \underline{\mathbf{C}}^{B/A})^{-1} - f_B \underline{\mathbf{t}}^A \right)^{-1} \right)^{-1} - f_C \underline{\mathbf{t}}^B \right)^{-1},$$

where $f_{AB} = (F_A + F_B) / (F_A + F_B + F_C) = 1 - f_C$. A third lamination orientation (C) for a fourth matrix phase of (D) planes in which the (ABC) medium is embedded yields in turn:

$$\underline{\mathbf{C}}^{ABCD} = \underline{\mathbf{C}}^D - f_{ABC} \left(\left(\Delta \underline{\mathbf{C}}^{D/C} + \left(\Delta \underline{\mathbf{C}}^{C/B} + f_A \left((\Delta \underline{\mathbf{C}}^{B/A})^{-1} - f_B \underline{\mathbf{t}}^A \right)^{-1} - f_C \underline{\mathbf{t}}^B \right)^{-1} \right)^{-1} - f_D \underline{\mathbf{t}}^C \right)^{-1},$$

as $\mathbf{C}_{3\text{-HML}}^{\text{eff}}$, with $f_{ABC} = F_A + F_B + F_C = 1 - f_D = 1 - F_D$. The related stress increments in the A, B, C, D phases read as

$$\begin{aligned}\underline{\underline{\mathbf{d}\sigma}}^{(A)} &= \underline{\underline{\mathbf{B}}}^A : \underline{\underline{\mathbf{d}\sigma}}^{(AB)} + (f_B) \underline{\underline{\mathbf{F}}}^A : \left(\underline{\underline{\mathbf{d}\varepsilon}}^{P(A)} - \underline{\underline{\mathbf{d}\varepsilon}}^{P(B)} \right), \\ \underline{\underline{\mathbf{d}\sigma}}^{(B)} &= \underline{\underline{\mathbf{B}}}^B : \underline{\underline{\mathbf{d}\sigma}}^{(AB)} - (1 - f_B) \underline{\underline{\mathbf{F}}}^A : \left(\underline{\underline{\mathbf{d}\varepsilon}}^{P(A)} - \underline{\underline{\mathbf{d}\varepsilon}}^{P(B)} \right), \\ \underline{\underline{\mathbf{d}\sigma}}^{(C)} &= \underline{\underline{\mathbf{B}}}^C : \underline{\underline{\mathbf{d}\sigma}}^{(ABC)} - (1 - f_C) \underline{\underline{\mathbf{F}}}^B : \left(\underline{\underline{\mathbf{d}\varepsilon}}^{P(AB)} - \underline{\underline{\mathbf{d}\varepsilon}}^{P(C)} \right), \\ \underline{\underline{\mathbf{d}\sigma}}^{(D)} &= \underline{\underline{\mathbf{B}}}^D : \underline{\underline{\mathbf{d}\Sigma}} - (1 - f_D) \underline{\underline{\mathbf{F}}}^C : \left(\underline{\underline{\mathbf{d}\varepsilon}}^{P(ABC)} - \underline{\underline{\mathbf{d}\varepsilon}}^{P(D)} \right),\end{aligned}$$

with

$$\begin{aligned}\underline{\underline{\mathbf{d}\sigma}}^{(AB)} &= \underline{\underline{\mathbf{B}}}^{AB} : \underline{\underline{\mathbf{d}\sigma}}^{(ABC)} + (f_C) \underline{\underline{\mathbf{F}}}^B : \left(\underline{\underline{\mathbf{d}\varepsilon}}^{P(AB)} - \underline{\underline{\mathbf{d}\varepsilon}}^{P(C)} \right), \\ \underline{\underline{\mathbf{d}\sigma}}^{(ABC)} &= \underline{\underline{\mathbf{B}}}^{ABC} : \underline{\underline{\mathbf{d}\Sigma}} + (f_D) \underline{\underline{\mathbf{F}}}^C : \left(\underline{\underline{\mathbf{d}\varepsilon}}^{P(ABC)} - \underline{\underline{\mathbf{d}\varepsilon}}^{P(D)} \right) \quad \text{and} \\ \underline{\underline{\mathbf{d}\varepsilon}}^{P(AB)} &= f_B \underline{\underline{\mathbf{B}}}^{tB} : \underline{\underline{\mathbf{d}\varepsilon}}^{P(B)} + (1 - f_B) \underline{\underline{\mathbf{B}}}^{tA} : \underline{\underline{\mathbf{d}\varepsilon}}^{P(A)}, \\ \underline{\underline{\mathbf{d}\varepsilon}}^{P(ABC)} &= (1 - f_C) \underline{\underline{\mathbf{B}}}^{tAB} : \left(f_B \underline{\underline{\mathbf{B}}}^{tB} : \underline{\underline{\mathbf{d}\varepsilon}}^{P(B)} + (1 - f_B) \underline{\underline{\mathbf{B}}}^{tA} : \underline{\underline{\mathbf{d}\varepsilon}}^{P(A)} \right) + f_C \underline{\underline{\mathbf{B}}}^{tC} : \underline{\underline{\mathbf{d}\varepsilon}}^{P(C)}.\end{aligned}$$

Connecting the stress increments $\underline{\underline{\mathbf{d}\sigma}}^{(\pi)}$ to the plastic strain increments $\underline{\underline{\mathbf{d}\varepsilon}}^{P(\pi')}$ yields the operators $\underline{\underline{\mathbf{B}}}^\pi$ and $\underline{\underline{\mathbf{F}}}^{\pi\pi'}$ for the (3)-HML intra-crystalline structure $A|B|C|(D)$, i.e. the operators $\underline{\underline{\mathbf{B}}}^{\alpha(I)}$ and $\underline{\underline{\mathbf{F}}}^{\alpha(I)\beta(I)}$ that enter Eq. (21) for a domain (I). Each operator $\underline{\underline{\mathbf{F}}}^{\pi\pi'}$, $\pi, \pi' = A, B, C, D$, takes the form of a linear combination of the $\underline{\underline{\mathbf{F}}}^{\pi''}$ operators, with $\pi'' = A, B, C$. For homogeneous elasticity, $\underline{\underline{\mathbf{B}}}^\pi = \underline{\underline{\mathbf{I}}}$ yields $\underline{\underline{\mathbf{F}}}^{\pi''} = -\underline{\underline{\mathbf{t}}}^{\pi''}$ (Appendix A). The operators $\underline{\underline{\mathbf{F}}}^{\pi\pi'} = \sum_{\pi''} \phi_{\pi''}^{\pi\pi'} \underline{\underline{\mathbf{F}}}^{\pi''} = -\sum_{\pi''} \phi_{\pi''}^{\pi\pi'} \underline{\underline{\mathbf{t}}}^{\pi''}$ are given in Table 2.

References

- Acharya, A., Bassani, J.L., 2000. Lattice incompatibility and a gradient theory of crystal plasticity. *J. Mech. Phys. Solids* 48, 1565–1595.
- Althoff, J., Wincierz, P., 1972. The influence of texture on the yield loci of copper and aluminium. *Z. Metallkd.* 63, 623–633.
- Arminjon, M., 1991. A regular form of the Schmid law, application to the ambiguity problem. *Texture Microstruct.* 14–18, 1121–1128.
- Asaro, R.J., Needleman, A., 1985. Texture development and strain hardening in rate dependent poly-crystals. *Acta Metallurgica* 33 (6), 923–940.
- Bassani, J.L., Wu, T.Y., 1991. Latent hardening in single crystals. I. Theory and experiments. *Proc. R. Soc. London A* 435, 21–41.
- Berbenni, S., Franciosi, P., 2004. Yield surfaces using an extension of the “Regularized” Schmid Law to polycrystalline materials. In: Gutkowski, W., Kowalewski, T.A. (Eds.), *Proceedings of the 21th International Congress of Theoretical and Applied Mechanics—IUTAM Symposium, 15–21 August 2004, Warsaw, Poland.*
- Berbenni, S., Favier, V., Lemoine, X., Berveiller, M., 2004. Micromechanical modeling of the elastic-viscoplastic behavior of steels having different microstructures. *Mater. Sci. Eng. A* 372, 128–136.

- Berryman, J.G., 2004. Bounds on elastic constants for random polycrystals of laminates. *J. Appl. Phys.* 96 (8), 4281–4287.
- Berveiller, M., Muller, D., Kratochvil, J., 1993. Non local versus local elastoplastic behavior of heterogeneous materials. *Int. J. Plast.* 9 (5), 633–652.
- Bishop, J.F.W., Hill, R., 1951. A theory of the plastic distortion of a poly-crystalline aggregate under combined stresses. *Philos. Mag.* 42, 414–427.
- Bunge, H.-J., 1982. *Texture Analysis in Materials Science—Mathematical Methods*. Butterworths, London.
- Chaboche, J.-L., Kruch, S., Maire, J.-F., Pottier, T., 2001. Towards a micromechanics based inelastic and damage modeling of composites. *Int. J. Plast.* 17, 411–439.
- Darrieulat, M., Piot, D., 1996. A method of generating analytical yield surfaces of crystalline materials. *Int. J. Plast.* 12 (5), 575–610.
- Dvorak, G.J., 1992. Transformation field analysis in inelastic composite materials. *Proc. R. Soc. London A* 437, 311–327.
- Dvorak, G.J., Bahei-El-Din, A., 1997. Inelastic composite materials: transformation field analysis and experiments. In: Suquet, P. (Ed.), *Continuum Micromechanics, CISM Course and Lecture 377*. Springer, Berlin, pp. 1–59.
- Dvorak, G.J., Benveniste, Y., 1992. On transformation strains and uniform fields in multiphase elastic media. *Proc. R. Soc. London A* 437, 291–310.
- Eshelby, J.D., 1957. The determination of the elastic field of an ellipsoidal inclusions and related problems. *Proc. R. Soc. London A* 421, 376–396.
- Estevez, R., Hoinard, G., Franciosi, P., 1997. Hardening anisotropy of γ/γ' superalloy single crystals. *Acta Mater.* 45, 1567–1584.
- Fish, J., Shek, K., 1999. Finite deformation plasticity for composite structures: computational models and adaptative strategies. *Comput. Method Appl. Mech. Eng.* 172, 145–174.
- Fleck, N.A., Muller, G.M., Ashby, M.F., Hutchinson, J.W., 1994. Strain gradient plasticity: theory and experiment. *Acta Metallurgica Mater.* 42 (2), 475–487.
- Francfort, G., Murat, F., 1986. Homogenization and optimal bounds in linear elasticity. *Arch. Ration. Mech. Anal.* 94, 307–334.
- Franciosi, P., 1985. The concepts of latent hardening and strain hardening in metallic single crystals. *Acta Metallurgica* 33 (9), 1601–1612.
- Franciosi, P., 1988. On flow and work hardening expression correlations in metallic single crystal plasticity. *Rev. Phys. Appl.* 23, 383–394.
- Franciosi, P., 1994. Introduction of equivalent deformation mechanisms for the description of FCC crystals post-stage II plasticity kinematics. *Key Eng. Mater.* 97 (9), 323–328.
- Franciosi, P., Berbenni, S., 2005. regularized Schmid law in metal plasticity: from single to poly-crystals. In: Khan, A.S. (Ed.), *Proceedings of the 11th International Symposium on Plasticity and its Current Applications*, 3–9 January 2005, Hawaii, USA.
- Franciosi, P., Berbenni, S., 2006. About the use of a Regularized Schmid flow criterion in polycrystal plasticity TFA-modeling. In: Khan, A.S. (Ed.), *Proceedings of the 12th International Symposium on Plasticity and its Current Applications*, July 2006, Halifax, Canada.
- Franciosi, P., Lormand, G., 2004. Using the Radon transform method to solve inclusion problems in elasticity. *Int. J. Solid Struct.* 41 (3/4), 585–606.
- Franciosi, P., Zaoui, A., 1991. Crystal hardening and the issue of uniqueness. *Int. J. Plast.* 7, 295–311.
- Gambin, W., 1991. Plasticity of crystals with interacting slip systems. *Eng. Trans.* 39 (3/4), 303–324.
- Gambin, W., 1992. Refined analysis of elastic plastic crystals. *Int. J. Solid Struct.* 29, 2013–2021.
- Havner, K.S., 1973. On the mechanics of crystalline solids. *J. Mech. Phys. Solids* 21, 383–394.
- Hill, R., 1965. Continuum micro-mechanics of elastoplastic poly-crystals. *J. Mech. Phys. Solids* 13, 89–101.
- Hill, R., Rice, J.R., 1972. Constitutive analysis of elastic-plastic crystals at arbitrary strains. *J. Mech. Phys. Solids* 20 (6), 401–413.
- Imbault, D., Arminjon, M., 1998. Deformation textures of fcc materials predicted with a regular form of the Schmid law. *Mater. Sci. Forum* 273–275, 371–376.
- Kocks, U.F., Franciosi, P., Kawai, M., 1991. A forest model of latent hardening and its application to polycrystal deformation. *Texture Microstruct.* 14–18, 1103–1114.
- Kowalczyk, K., Gambin, W., 2004. Model of plastic anisotropy evolution with texture dependent yield surface. *Int. J. Plast.* 20, 19–54.
- Kröner, E., 1961. Zur Plastischen Verformung des Vielkristalls. *Acta Metallurgica* 9, 155–161.

- Kulhmann-Wilsdorf, D., 2002. Why do dislocations assemble into interfaces in epitaxy as well as in crystal plasticity? To minimize free energy. *Metall. Mater. Trans. A* 33 (8/1), 2519–2539.
- Levin, V.M., 1967. Thermal expansion coefficients for heterogeneous materials. *Mekhanika Tverdogo Tela* 2, 88–94 (English translation: *Mechanics of Solids* 11, 58–61).
- Li, J., Weng, G.J., 1997. A secant-viscosity approach to the time-dependent creep of an elastic-viscoplastic composite. *J. Mech. Phys. Solids* 45, 1069–1083.
- Luskin, M., 1996. Approximation of laminated microstructures for a rotationally invariant double well energy density. *Numer. Math.* 75, 205–221.
- Madec, R., Devincere, B., Kubin, L., Hoc, T., Rodney, D., 2003. The role of collinear interaction in dislocation-induced hardening. *Science* 301, 1879–1882.
- Masson, R., Bornert, M., Suquet, P., Zaoui, A., 2000. An affine formulation for the prediction of the effective properties of non linear composites and poly-crystals. *J. Mech. Phys. Solids* 48 (6/7), 1203–1227.
- Mecif, A., Bacroix, B., Franciosi, P., 1997. Temperature and orientation dependent plasticity features of Cu and Al single crystals under axial compression. *Acta Materialia* 45 (1), 371–381.
- Michel, J.C., Suquet, P., 2003. Non uniform transformation field analysis. *Int. J. Solid Struct.* 40, 6937–6955.
- Michel, J.C., Suquet, P., 2004. Computational analysis of nonlinear composite structures using the non uniform transformation field analysis. *Comput. Method Appl. Mech. Eng.* 193, 5477–5502.
- Milton, G.W., 1988. Classical Hall effect in two-dimensional composites: a characterization of the set of realizable effective conductivity tensors. *Phys. Rev. B* 38 (16), 11296–11303.
- Ortiz, M., Repetto, E.A., 1999. Non convex energy minimization and dislocation structures in ductile single crystals. *J. Mech. Phys. Solids* 47, 397–462.
- Ortiz, M., Repetto, E.A., Stainier, L., 2000. A theory of sub-grain dislocation structures. *J. Mech. Phys. Solids* 48, 2077–2114.
- Ponte-Castaneda, P., Suquet, P., 1998. Non linear composites. *Adv. Appl. Mech.* 34, 172–302.
- Ponte-Castaneda, P., Willis, J.R., 1995. The effect of spatial distribution on the effective behavior of composite materials and cracked media. *J. Mech. Phys. Solids* 43, 1919–1951.
- Sabar, H., Berveiller, M., Favier, V., Berbenni, S., 2002. A new class of micro-macro models for elastic-viscoplastic heterogeneous materials. *Int. J. Solid Struct.* 39 (12), 3257–3276.
- Sarma, G.B., Radhakrishnan, B., Dawson, P.R., 2002. Mesoscale modeling of microstructure and texture evolution during deformation processing of metals. *Adv. Eng. Mater.* 4 (7), 509–514.
- Suquet, P., 1997. Effective behavior of non linear composites. In: Suquet, P. (Ed.), *Continuum Micromechanics, CISM course and lecture 377*. Springer, Berlin, pp. 220–259.